

## Benchmarking Atomic Data for Astrophysics: Be-like Ions between B II and Ne VII

KAI WANG,<sup>1,2,3</sup> ZHAN BIN CHEN,<sup>4</sup> CHUN YU ZHANG,<sup>3</sup> RAN SI,<sup>3</sup> PER JÖNSSON,<sup>2</sup> HENRIK HARTMAN,<sup>2</sup> MING FENG GU,<sup>5</sup> CHONG YANG CHEN,<sup>3</sup> AND JUN YAN<sup>6,7,8</sup>

<sup>1</sup>*Hebei Key Lab of Optic-electronic Information and Materials, The College of Physics Science and Technology, Hebei University, Baoding 071002, China;*

<sup>2</sup>*Group for Materials Science and Applied Mathematics, Malmö University, SE-20506, Malmö, Sweden; per.jonsson@mah.se*

<sup>3</sup>*Shanghai EBIT Lab, Key Laboratory of Nuclear Physics and Ion-beam Application, Institute of Modern Physics, Department of Nuclear Science and Technology, Fudan University, Shanghai 200433, China; chychen@fudan.edu.cn*

<sup>4</sup>*College of Science, Hunan University of Technology, Zhuzhou 412000, China*

<sup>5</sup>*Space Science Laboratory, University of California, Berkeley, CA 94720, USA*

<sup>6</sup>*Institute of Applied Physics and Computational Mathematics, Beijing 100088, China; yan\_jun@iapcm.ac.cn*

<sup>7</sup>*Center for Applied Physics and Technology, Peking University, Beijing 100871, China;*

<sup>8</sup>*Collaborative Innovation Center of IFSA (CICIFSA), Shanghai Jiao Tong University, Shanghai 200240, China*

Submitted to ApJS

### ABSTRACT

Large-scale self-consistent multiconfiguration Dirac–Hartree–Fock and relativistic configuration interaction calculations are reported for the  $n \leq 6$  levels in Be-like ions from B II to Ne VII. Effects from electron correlation are taken into account by means of large expansions in terms of a basis of configuration state functions, and a complete and accurate data set of excitation energies, lifetimes, wavelengths, and electric dipole, magnetic dipole, electric quadrupole, and magnetic quadrupole line strengths, transition rates, and oscillator strengths for these levels is provided for each ion. Comparisons are made with available experimental and theoretical results. The uncertainty of excitation energies is assessed to be 0.01% on average, which makes it possible to find and rule out misidentifications and aid new line identifications involving high-lying levels in astrophysical spectra. The complete data set is also useful for modeling and diagnosing astrophysical plasmas.

*Keywords:* atomic data - atomic processes

## 1. INTRODUCTION

A wealth of astrophysical spectra has been obtained from different missions, such as Chandra, X-ray Multi-Mirror Mission (XMM-Newton), Hinode, and Hard X-ray Modulation Telescope (HXMT). The analysis of these expensively acquired spectra is often not limited by the capabilities of the spectrometers themselves, but by the lack of accurate reference data in the atomic line database (Bigot & Thévenin 2006; Kallman & Palmeri 2007; Ruffoni et al. 2013). To solve this dilemma, we have computed highly accurate energy and radiative transition data for L-shell atomic ions (Jönsson et al. 2013; Ekman et al. 2014; Wang et al. 2014, 2015, 2016a,b, 2017c; Radžiūtė et al. 2015; Si et al. 2016). This work reports accurate atomic data resulting from our systematic calculations for beryllium-like ions from B II to Ne VII.

These ions have been observed in spectra from different astrophysical objects, such as the sun (Curdt et al. 1997, 2001, 2004; Feldman et al. 1997; Del Zanna & Andretta 2011; Ko et al. 2002; Parenti et al. 2005; Tian et al. 2009; Thomas & Neupert 1994), white dwarfs (Raassen et al. 2002; Werner et al. 2004), as well as nebular regions in RR Tel (Penston & Lago 1983). The atomic lines do not only tell what elements are present in astrophysical objects and what are their relative abundances, but also reveal the physical conditions in the plasmas, such as density, temperature and radiation fields, along with important excitation mechanisms and photo-processes. For example, the  $n = 3 \rightarrow 2$  O V lines identified by the Extreme Ultraviolet (EUV) Imaging Spectrometer of the Hinode are density sensitive and can be used for density diagnostics of the solar corona (Landi & Young 2009). C III lines have been observed in NGC 2440 and provided carbon abundance information for this planetary nebula (Rubin et al. 2004). Due to the high cosmic abundance from these light elements, the lines often appear strong, increasing their value as probes of physical conditions.

Atomic data for low-lying levels ( $1s^2$ ) $2l^2$  and  $2l3l'$  with  $l \leq 1$  and  $l' \leq 2$  (the  $n = 2, 3$  complexes) of the ions from B II to Ne VII have previously been obtained from different calculations (Safranova et al. 1996, 1997, 1999; Tachiev & Froese Fischer 1999; Komasa et al. 2002; Gálvez et al. 2003; Froese Fischer & Tachiev 2004; Gu 2005a; Ho et al. 2006; Cheng et al. 2008; Marques et al. 2012; Verdebout et al. 2014). For many objects, however, emission lines from higher-excitation lines are observed. In the spectrum of the active Seyfert Galaxy NGC 1068 (Brinkman) and the supergiant  $\delta$  Orionis (Raassen & Pollock 2013), lines from levels with  $n > 3$  in the light elements such as C, N, O are identified.

There is thus a need for corresponding atomic data for the  $n > 3$  higher-lying levels to be provided. Our present study is improving existing data, and extending the included levels to  $n \leq 6$  as is described below. The new data will extend the probes of physical conditions in different astrophysical objects, as well as of analyzing new observations from different space missions and laboratory experiments (Träbert et al. 2014a,b).

The energies for the  $2lnl' \ ^1S$  ( $n = 2 - 6$ ) states and transition rates for the  $2lnl' \ ^1S - 2s2p \ ^1P$  transition were calculated by Zhang & Gou (2005) for the beryllium isoelectronic sequence ( $Z = 4 - 10$ ) using a configuration interaction method. Excitation energies of the  $2pns \ ^1,3P$  and  $2pnd \ ^1,3P$  Rydberg states ( $n = 3 - 60$ ) in B II were semi-empirically determined by Sakho et al. (2013) in the framework of the screening-constant-by-unit-nuclear-charge method. Savukov & Markhotok (2006) performed many-body perturbation theory (MBPT) calculations for a large number of energy levels in Be-like Ne VII. The AUTOSTRUCTURE calculations of Fernández-Menchero et al. (2014) were performed for the  $n > 3$  levels of Be-like ions with  $Z \leq 10$ . Data for the  $n > 3$  states of N IV were provided by Aggarwal et al. (2016) using the GRASP0 code (Grant et al. 1980), and by Fernández-Menchero et al. (2017) using the B-spline box-based close-coupling method (Zatsarinny & Froese Fischer 2009).

Among the different studies involving the  $n > 3$  levels the one by Savukov & Markhotok (2006) for Ne VII provides energy data of high accuracy. In comparison, although complete sets of data including transition rates are provided, the studies by Fernández-Menchero et al. (2014), for the ions with  $Z = 5 - 10$ , and by Aggarwal et al. (2016) and Fernández-Menchero et al. (2017), for N IV, are quite inaccurate because of limited configuration interaction effects included in the calculations. For example, the excitation energies of Fernández-Menchero et al. (2014), Aggarwal et al. (2016), and Fernández-Menchero et al. (2017) for N IV depart from the experimental energies compiled in the Atomic Spectra Database (ASD) of the National Institute of Standards and Technology (NIST) (Kramida et al. 2016) by up to 5.8%, 5.7%, and 2.4%, respectively. These uncertainties are too large for identification and deblending of new observations from different space missions.

To fill the gaps of lacking accurate atomic data for high-lying states of the ions from B II to Ne VII, in particular accurate transition rates, we performed large-scale multiconfiguration Dirac–Hartree–Fock (MCDHF) and relativistic configuration interaction (RCI) calculations using the latest version of the GRASP2K

code (Jönsson et al. 2013). The calculations provide a consistent and highly accurate data set of energy structure and radiative transition parameters involving also the  $n > 3$  levels for these low charged Be-like ions. This work is a continuation of our previous calculations (Wang et al. 2015), in which the corresponding accurate results are reported for the ions in the range of nuclear charges  $10 \leq Z \leq 36$ . The excitation energies and lifetimes for the levels of the  $2l^2$  (with  $l \leq 1$ ) and  $2lnl'$  (with  $n \leq 6$  and  $l' \leq n - 1$ ) configurations, which are below the levels of the  $2s7l$  configuration, and electric dipole (E1), magnetic dipole (M1), electric quadrupole (E2), and magnetic quadrupole (M2) transition rates among these states are calculated for each ion. To assess the accuracy of the present MCDHF/RCI data, MBPT calculations for Ne VII are carried out using the Flexible Atomic Code (FAC) (Gu 2008). The two sets of results are in excellent agreement. Compared with previous calculations of Be-like ions, the present work results in a significant extension of accurate energy and transition data for higher-lying states of the  $n > 3$  configurations, which will greatly aid the analysis of new spectra from astrophysical sources, as well as improving the assessment of blending for diagnostic lines of interest.

## 2. THEORY AND CALCULATIONS

### 2.1. MCDHF

The MCDHF method has been described in detail by Grant (2007) and Froese Fischer et al. (2016). The method is also outlined in our previous calculations (Jönsson et al. 2013; Ekman et al. 2014; Wang et al. 2016a,b, 2017c,a,b; Radžiūtė et al. 2015; Si et al. 2016; Chen & Wang 2017; Chen et al. 2017). Based on the active space (AS) approach (Olsen et al. 1988; Sturesson et al. 2007) for the generation of the configuration state function (CSF) expansions, separate calculations are done for the even and odd parity states. For the even parity states, the CSF expansions are obtained by allowing single and double (SD) excitations from the multi-reference (MR) configurations  $2s^2$ ,  $2p^2$ ,  $2s3s$ ,  $2s3d$ ,  $2p3p$ ,  $2s4s$ ,  $2s4d$ ,  $2p4p$ ,  $2p4f$ ,  $2s5s$ ,  $2s5d$ ,  $2s5g$ ,  $2p5p$ ,  $2p5f$ ,  $2s6s$ ,  $2s6d$ ,  $2s6g$ ,  $2p6p$ ,  $2p6f$ , and  $2p6h$  to an AS of orbitals. For the odd parity states, the CSF expansions are obtained by allowing SD excitations from the MR configurations  $2s2p$ ,  $2s3p$ ,  $2p3s$ ,  $2p3d$ ,  $2s4p$ ,  $2s4f$ ,  $2p4s$ ,  $2p4d$ ,  $2s5p$ ,  $2s5f$ ,  $2p5s$ ,  $2p5d$ ,  $2p5g$ ,  $2s6p$ ,  $2s6f$ ,  $2s6h$ ,  $2p6s$ ,  $2p6d$ , and  $2p6g$  to an AS of orbitals. In the first step of the calculations, the AS is

$$\text{AS}_1 = \{7s, 7p, 7d, 7f, 7g, 7h, 7i\}.$$

Then, the AS is increased in the following way:

$$\text{AS}_2 = \text{AS}_1 + \{8s, 8p, 8d, 8f, 8g, 8h, 8i, 8k\},$$

$$\text{AS}_3 = \text{AS}_2 + \{9s, 9p, 9d, 9f, 9g, 9h, 9i, 9k\},$$

$$\text{AS}_4 = \text{AS}_3 + \{10s, 10p, 10d, 10f, 10g, 10h, 10i, 10k\},$$

$$\text{AS}_5 = \text{AS}_4 + \{11s, 11p, 11d, 11f, 11g, 11h, 11i, 11k\}$$

SD excitations from the  $1s$  subshell to active sets with principal quantum numbers  $n \leq 7$  are allowed, whereas at most one excitation from the  $1s$  subshell is allowed to active sets with principal quantum numbers  $8 \leq n \leq 11$ . The final model using the  $\text{AS}_5$  active set contains 777 325 even and 800 410 odd parity CSFs. The Breit interaction and leading QED effects (vacuum polarization and self-energy) are included in subsequent RCI calculations. All calculations were performed using the GRASP2K code (Jönsson et al. 2007; Jönsson et al. 2013).

### 2.2. MBPT

The MBPT method is explained in Lindgren (1974); Safranova et al. (1996); Vilkas et al. (1999); Gu (2005b, 2007), and it has been implemented in the FAC package (Gu 2008). The key feature of the MBPT method is the partitioning of the Hilbert space of the system into two subspaces, the model space  $M$  and the orthogonal space  $O$ . The configuration interaction effects in the  $M$  space are exactly considered, while the interaction between the space  $M$  and  $O$  is taken into account with the second-order perturbation method. For the MBPT calculation, the model space  $M$  contains the even and odd multi-reference configurations of the MCDHF/RCI method, while the space  $O$  contains all the possible configurations that are generated by SD virtual excitations of the  $O$  space. For single and double excitations, the maximum  $n$  values are 125 and 65, respectively, with a maximum  $l$  value of 25. Just as for the MCDHF/RCI calculations, QED effects are also included.

## 3. EVALUATION OF DATA

### 3.1. Energy Levels

The excitation energies for the lowest 138 states of the  $2s^2$ ,  $2p^2$  and  $2lnl'$  (with  $n \leq 6$ , with  $l \leq 1$  and  $l' \leq n - 1$ ) configurations with  $Z = 8 - 10$  from our MCDHF/RCI calculations are listed in Table 1, along with the results for the lowest 100 states of these configurations with  $Z = 5 - 7$ . All these levels are below the levels of the  $2s7l$  configurations. In relativistic calculations the wave functions for the states are given as

expansions over  $jj$ -coupled CSFs. This labeling system is rarely used in databases or by experimentalists. To overcome this labeling problem, the method developed [Gaigalas et al. \(2004\)](#); [Gaigalas et al. \(2017\)](#) is used to transform wave functions from the  $jj$ -coupling to the  $LSJ$ -coupling scheme. In Table 1, for each level numbered by a key (#), the  $LSJ$  designation, the total angular momentum and parity  $J^\pi$ , and the radiative lifetime estimated from theoretical transition rates are also included.

Among the six Be-like ions considered here, both experimental and theoretical energy data of the levels up to the  $n = 6$  configurations are relatively complete for Ne VII. In what follows we will firstly access the accuracy of the MCDHF/RCI excitation energies for Ne VII, by comparing available results. In Table 2, we present the MCDHF/RCI excitation energies of the 138 levels for Ne VII as a function of the increasing active set (AS). For comparison, the compiled values from the NIST ASD ([Kramida et al. 2016](#)) are given as well. The mean differences between the MCDHF/RCI and NIST excitation energies and the corresponding standard deviations are  $-868 \pm 1724 \text{ cm}^{-1}$ ,  $-439 \pm 625 \text{ cm}^{-1}$ ,  $-240 \pm 264 \text{ cm}^{-1}$ ,  $-179 \pm 219$ , and  $-170 \pm 206 \text{ cm}^{-1}$  for the calculations based on AS<sub>1</sub>, AS<sub>2</sub>, AS<sub>3</sub>, AS<sub>4</sub>, and AS<sub>5</sub>, respectively. This implies that the MCDHF/RCI calculations are well converged with respect to an increasing size of the AS and that the accuracy cannot be further improved by extending the orbital set. Remaining energy differences are due to higher order correlation effects not captured within the framework of SD excitation from the MR. For AS<sub>5</sub> the standard deviation given above corresponds to an average relative difference of  $-0.01\% \pm 0.02\%$ .

In Table 3, computed excitation energies of Ne VII from the present MCDHF/RCI and MBPT calculations and from the calculations by [Savukov & Markhotok \(2006\)](#) [hereafter referred to as MBPT2], [Tachiev & Froese Fischer \(1999\)](#); [Froese Fischer & Tachiev \(2004\)](#) [MCHF/BP], [Safranova et al. \(1996, 1997\)](#) [MBPT3], and by [Fernández-Menchero et al. \(2014\)](#) [AUTOSTRUCTURE] are compared with the NIST compiled values. The present MBPT calculations used the same method and code as in [Wang et al. \(2015\)](#) and [Gu \(2005a\)](#). Due to these similarities, the latter results are not shown in Table 3.

Compared with the MBPT3 and MCHF/BP calculations, the present MCDHF/RCI and MBPT calculations, as well as the MBPT2 calculations, report data for higher states. Moreover, the latter three calculations show better agreement with the NIST experimental values. The average differences with the standard devia-

tions between the computed excitation energies and the NIST values for the  $n \leq 3$  levels are  $-129 \pm 174 \text{ cm}^{-1}$  for MCDHF/RCI,  $-134 \pm 281 \text{ cm}^{-1}$  for MBPT, and  $100 \pm 372 \text{ cm}^{-1}$  for MBPT2. The corresponding values for MBPT3 and MCHF/BP are  $-303 \pm 609 \text{ cm}^{-1}$  and  $468 \pm 211 \text{ cm}^{-1}$ , respectively.

Inspecting all the  $n \leq 6$  results of the MCDHF/RCI, MBPT, and MBPT2 calculations for Ne VII more carefully, one can see that the accuracies of three different calculations, for which the relative average energy differences with the NIST values are  $-0.01\% \pm 0.02\%$  (MCDHF/RCI),  $-0.01\% \pm 0.03\%$  (MBPT), and  $0.01\% \pm 0.06\%$  (MBPT2), respectively, are generally at the same level. The largest deviations with the NIST values are  $-776 \text{ cm}^{-1}$  for #122/2s6p  $^1P_1$  of MCDHF/RCI,  $-1111 \text{ cm}^{-1}$  for #37/2p3p  $^1D_2$  of MBPT, and  $2102 \text{ cm}^{-1}$  #10/2p $^2$   $^1S_0$  of MBPT2. In comparison, although providing complete sets of energy data along with collision strengths, the AUTOSTRUCTURE calculations ([Fernández-Menchero et al. 2014](#)), show a much larger average difference with the NIST values,  $-2229 \pm 2625 \text{ cm}^{-1}$ , which is far greater than the requirement of analyses of new astrophysical spectra.

Experimental and theoretical energy data are available for many  $n \leq 3$  levels along the isoelectronic sequence from B II to Ne VII. To further assess the accuracy of our computed energy values, a comparison with the NIST experimental values as well as with values from the MBPT3 and MCHF/BP calculations, is given in Table 4. From the table it is clear that the present MCDHF/RCI calculations provide more theoretical data compared with the two previous calculations. The differences with the NIST experimental values are also much smaller for our calculations than those from the MBPT3 and MCHF/BP calculations. More specifically, excluding the levels 2p3p  $^3S_1$  with  $Z = 5, 7$ , 2p3d  $^3P_0^\circ$  with  $Z = 5$ , and 2p3p  $^1S_0$  with  $Z = 9$ , for which the differences of theory from experiment are greater than  $1000 \text{ cm}^{-1}$  (they will be further discussed below), the average differences with standard deviations,  $\Delta E \pm \sigma$ , with the NIST values are  $-23 \pm 141 \text{ cm}^{-1}$  for MCDHF/RCI,  $-630 \pm 1854 \text{ cm}^{-1}$  for MBPT3, and  $256 \pm 173 \text{ cm}^{-1}$  for MCHF/BP. It should be noted that the differences of the MBPT3 and NIST values decrease with increasing  $Z$  for the same level and that the large uncertainties for this method mainly come from the low-charge ions.

Among the levels 2p3p  $^3S_1$  at  $Z = 5, 7$ , 2p3d  $^3P_0^\circ$  at  $Z = 5$ , and 2p3p  $^1S_0$  at  $Z = 9$ , where the differences of the MCDHF/RCI and NIST values are greater than  $1000 \text{ cm}^{-1}$ , the largest difference is  $-10451.5 \text{ cm}^{-1}$  for the level #29/2p3p  $^3S_1$  at  $Z = 7$ . The NIST en-

ergy  $498045.5 \text{ cm}^{-1}$  for this level is in good agreement with our MCDHF/RCI value  $498010 \text{ cm}^{-1}$  for the level #37/ $2s4s\ ^3S_1$ . From Table 1 we can see that the weights for the first two eigenvector components of the level #29 are 70 % ( $2p3p\ ^3S_1$ ) and 27 % ( $2s4s\ ^3S$ ), whereas those of the level #37 are 72 % ( $2s4s\ ^3S$ ) and 27 % ( $2p3p\ ^3S_1$ ). The two levels with relatively pure  $LS$  coupling are mixed with each other, but the mixing is not strong. This implies that the NIST value  $498045.5 \text{ cm}^{-1}$  should be designated as the  $2s4s\ ^3S_1$  level. Apart from  $2p3p\ ^3S_1$  at  $Z = 7$ , we cannot find obvious alternate designations for the other three levels in the present MCDHF/RCI calculations. As an example, the energy differences for the  $2p3p\ ^3S_1$  and  $2p3d\ ^3P_0^\circ$  levels as a function of  $Z$  are shown in Figure 1. Two anomalies exist for the  $2p3p\ ^3S_1$  (the difference is  $1030.5 \text{ cm}^{-1}$ ) and  $2p3d\ ^3P_0^\circ$  ( $1989.4 \text{ cm}^{-1}$ ) levels at  $Z = 5$ . Because the same scheme is used for each ion in the present MCDHF/RCI calculations, ensuring that the accuracy of our values for the same level is systematic and consistent, the large differences for these states are caused by relatively large uncertainty of the NIST values.

Lastly we compare the MCDHF/RCI excitation energies for the  $n = 4 - 6$  levels from B II to Ne VII, which are not computed by Tachiev & Froese Fischer (1999); Froese Fischer & Tachiev (2004, MCHF/BP) nor by Safranova et al. (1996, 1997, MBPT3), with the experimental values from the NIST ASD. Removing 3 obvious outliers,  $\Delta E = 10\ 395.6, 2\ 659$ , and  $6\ 258 \text{ cm}^{-1}$  for the levels #37/ $2s4s\ ^3S_1$  with  $Z = 7$ , and #81/ $2p4s\ ^3P_2^\circ$  and #134/ $2p4p\ ^1S_0$  with  $Z = 8$ , respectively, we find that for the remaining  $n = 4 - 6$  levels in Table 1  $\Delta E \pm \sigma = -80 \pm 132 \text{ cm}^{-1}$ , which is highly satisfactory considering the range in excitation energy (exceeding  $1\ 500\ 000 \text{ cm}^{-1}$ ).

### 3.2. Transition rates

Table 5 lists transition rates  $A$  of the AS<sub>5</sub> active set for the E1, M1, E2, and M2 transitions connecting all the levels included in Table 1. To reduce the amount of data, only  $A$  values greater than  $10^{-5}$  times the sum of  $A$  values for all transitions from the upper level, i.e., radiative branching ratio (BR) greater than  $10^{-5}$ . Also included in this table are wavelengths  $\lambda$ , line strengths  $S$ , weighted oscillator strengths  $gf$ , and BR. The general rule is that transition data for electric multipoles (E1,E2) calculated in the Babushkin (length) gauge are preferable over transition data calculated in the Coulomb (velocity) gauge. Whereas generally true, recent work (Wang & Jönsson 2017; Pehlivan Rhodin et al. 2017) has shown that computed transition data from high states in neutral or near-

neutral systems are more stable and show better convergence properties with respect to the increasing active set of orbitals in the Coulomb gauge. For this reason, in Table 5, transition data from the  $n = 5, 6$  states in B II and C III are computed in the Coulomb gauge. Transitions from all other states are computed in the Babushkin gauge.

Since line strengths  $S$  for the transitions among the lowest 20 levels up to the  $2s3d$  configuration are provided by Tachiev & Froese Fischer (1999); Froese Fischer & Tachiev (2004) [MCHF/BP], available in the NIST ASD (Kramida et al. 2016), in Table 6 we compare these data with the values of the present MCDHF/RCI calculations using the AS<sub>5</sub> active set in Ne VII. Our MCDHF/RCI values of the AS<sub>4</sub> active set are also included in the table for comparison. Our two data sets (AS<sub>4</sub> and AS<sub>5</sub>) agree well within 3%, which indicates that the present MCDHF/RCI calculations using the AS<sub>5</sub> active set are well converged. The MCHF/BP values also show good agreement with our results except for the weak  $2s3s\ ^3S_1 - 2s2p\ ^1P_1^\circ$  and  $2s3d\ ^3D_1 - 2s2p\ ^1P_1^\circ$  intercombination transitions, which differ by more than 20%. It is also seen that transition data listed in the NIST ASD agree well with our results for most transitions. Differences larger than 20% occur for transitions of relatively small radiative branching ratios only, the transition  $2s3p\ ^3P_1^\circ - 2s^2\ ^1S_0$  being an exception. Although the  $S$  value for this transition is about  $5 \times 10^5$ , which is relatively small, the radiative branching ratio of this transition is 40.3%. This means that the above transition gives an important contribution to the lifetime of the level  $2s3p\ ^3P_1^\circ$ . An inspection of Table 6 reveals that the accuracy of the NIST values is overestimated for some transitions, especially for the transitions with the estimated accuracy A ( $\leq 3\%$ ), and the present MCDHF/RCI data should be more accurate than those listed in the NIST ASD.

To further access the accuracy of the present MCDHF/RCI transition data, in Figure 2, we compare the line strengths  $S$  from different resources (MCDHF/RCI (AS<sub>4</sub>), MCHF/BP, and NIST) with the results of the present MCDHF/RCI (AS<sub>5</sub>) calculations for the strong transitions with  $S \geq 10^{-2}$  among the lowest 20 levels up to the  $2s3d$  configuration for the ions from B II to Ne VII. Our two data sets (AS<sub>4</sub> and AS<sub>5</sub>) agree very well within 5% for all the transitions of the ions from B II to Ne VII, which again indicates that the present MCDHF/RCI calculations using the AS<sub>5</sub> active set are well converged. The MCHF/BP values also show good agreement with our results, within 10%, whereas the NIST values differ from the present calculations and the MCHF results by 10% - 60% for a few transitions. For

example, the MCDHF/RCI (AS<sub>4</sub>), MCDHF/RCI (AS<sub>5</sub>), and MCHF/BP values for the  $2s3p\ ^1P_1^{\circ} - 2p^2\ ^1S_0$  transition are  $7.34 \times 10^{-2}$ ,  $7.24 \times 10^{-2}$ , and  $7.20 \times 10^{-2}$ , respectively, while the corresponding NIST value is about 50% greater ( $1.09 \times 10^{-1}$ ). As a further check of the accuracy of the present transition data, we compare the  $S$  values of our MCDHF/RCI (AS<sub>4</sub>) and MCDHF/RCI (AS<sub>5</sub>) calculations for transitions involving highly-excited states above the  $2s3d$  configuration in Ne VII. Our two data sets agree within 10% for most of the transitions. However, large deviations sometimes occur for weak one-photon-two-electrons transitions <sup>1</sup>, which are generally very sensitive to electron correlation effects and sometimes to high-order relativistic effects.

### 3.3. Lifetimes

Lifetimes in Ne VII obtained in the Babushkin gauge in the current work (MCDHF/RCI (AS<sub>4</sub>) and reported by the MCHF/BP calculations (Tachiev & Froese Fischer 1999; Froese Fischer & Tachiev 2004) are compared with the MCDHF/RCI (AS<sub>5</sub>) calculations in Figure 3. To further check the accuracy of the MCDHF/RCI lifetimes, we also calculate the lifetimes in the Coulomb gauge using the present AS<sub>5</sub> model. The results are also included in Figure 3 for comparison. The agreement between the current lifetimes and the values reported by Tachiev & Froese Fischer (1999); Froese Fischer & Tachiev (2004) is very good, well within 5%. The differences of the present MCDHF/RCI (AS<sub>4</sub>) and MCDHF/RCI (AS<sub>5</sub>) calculations in the Babushkin gauge are within 5% for almost all levels, with the largest deviation of 6% for the level  $2s6s\ ^1S_0$ . The MCDHF/RCI (AS<sub>5</sub>) values in the Coulomb gauge also show good agreement (within 5%) with the Babushkin-gauge values from the same calculation, with the two exceptions:  $2s2p\ ^3P_1^{\circ}$  and  $2s6s\ ^1S_0$ . These two exceptions, with large deviations, occur for states with lifetimes determined by transitions with relatively small  $S$  values. For example, the lifetime of the level  $2s2p\ ^3P_1^{\circ}$  is determined by the weak intercombination transition  $2s2p\ ^3P_1^{\circ} - 2s^2\ ^1S_0$  with the  $S$  value of  $2 \times 10^{-5}$ . The contributions from the negative energy continuum, which are important for the transition rates in very weak intercombination transitions, are not included in the present MCDHF/RCI calculations in the Coulomb gauge. Therefore, the accuracy of the val-

ues in the Coulomb gauge, but not in the Babushkin gauge, are affected for the weak intercombination transition (Cheng et al. 2008).

Lastly we compare our MCDHF/RCI lifetimes in the Babushkin gauge with the experimental values from different sources and the MCDHF/RCI (Jönsson et al. 1998) and RCI (Cheng et al. 2008) calculations for the  $2s2p\ ^{1,3}P_1^{\circ}$  levels of the ions from B II to Ne VII. The agreement between the current lifetimes and lifetimes reported by different experimental and theoretical sources is surprisingly good for both the resonance transition  $2s2p\ ^1P_1^{\circ}$  and the intercombination transition  $2s2p\ ^3P_1^{\circ}$ . This is a strong indicator of the high accuracy of the present calculations.

### 3.4. Summary

Self-consistent MCDHF calculations and subsequent RCI calculations taking into account the Breit interaction and leading QED effects have been performed for the  $n \leq 6$  states of Be-like ions from B II to Ne VII. Level energies, transition energies, transition rates and lifetimes have been computed. Labeling of the states has been facilitated by converting from the  $jj$ -coupling to the  $LSJ$ -coupling scheme. Previous experimental and theoretical data involving low-lying  $n \leq 3$  states along the isoelectronic sequence, as well as both low-lying and high-lying states for Ne VII, are used to validate the present computations. An excellent agreement with experimental data is found, which is manifested by an average energy difference with the standard deviation for the  $n \leq 3$  states of only  $-23 \pm 141$  cm<sup>-1</sup> along the isoelectronic sequence. For all the 138 levels of Ne VII the average relative energy difference is  $-0.01 \% \pm 0.02 \%$ . Lifetimes in the Babushkin and Coulomb gauge agree to within 5% for most states of Ne VII. We have presented calculations for energy and transition data that are more extensive and accurate than previous work.

To summarize, the present work has significantly increased the amount of accurate data for the Be-like isoelectronic sequence, extending our previous calculations (Wang et al. 2015). The complete data set including both energy and transition results provided by the present work and by Wang et al. (2015) can be used for line identification and modeling purposes involving the  $n > 3$  high-lying states, which fills the gap for lacking accurate atomic data on Be-like ions. Our study can also be considered as a benchmark for other calculations.

## SCIENTIFIC SOFTWARE PACKAGES

Scientific software packages including

*Software:* GRASP2K (Jönsson et al. 2007; Jönsson et al. 2013) and FAC (Gu 2008) are used in the present work.

<sup>1</sup> A one-photon two-electron transition is a transition between states of configurations that differ by two electrons, e.g.  $2s^2\ ^1S_0 - 2p3d\ ^3P_1^{\circ}$ . The rates of these transitions are strictly zero in the lowest-order approximation of the calculation and attain non-zero values as basis functions are expanded to describe electron correlation (Li et al. 2010).

We thank the anonymous referee for many constructive comments on this manuscript. We acknowledge the support from the National Key Research and Development Program of China under Grant No. 2017YFA0403200, the National Natural Science Foundation of China (Grant Grant No. 11703004, No. 11674066, No. 11504421, and No. 11474034) and the Natural Science Foundation of Hebei Province, China (A2017201165). This work is also supported by the Swedish research council under contracts 2015-04842 and 2016-04185. The authors (K.W. and M.F.G.) express their gratitude to the support from the visiting researcher program at the Fudan University.

## REFERENCES

- Aggarwal, K. M., Keenan, F. P., & Lawson, K. D. 2016, MNRAS, 461, 3997
- Bashkin, S., McIntyre, L. C., Buttlar, H. v., Ekberg, J. O., & Martinson, I. 1985, Nuclear Instruments and Methods in Physics Research B, 9, 593
- Bigot, L., & Thévenin, F. 2006, MNRAS, 372, 609
- Chen, Z. B., Ma, K., Wang, H. J., et al. 2017, ADNDT, 113, 258
- Chen, Z. B., & Wang, K. 2017, ADNDT, 114, 61
- Cheng, K. T., Chen, M. H., & Johnson, W. R. 2008, PhRvA, 77, 052504
- Curdt, W., Brekke, P., Feldman, U., et al. 2001, A&A, 375, 591
- Curdt, W., Feldman, U., Laming, J. M., et al. 1997, A&AS, 126, 281
- Curdt, W., Landi, E., & Feldman, U. 2004, A&A, 427, 1045
- Del Zanna, G., & Andretta, V. 2011, A&A, 528, A139
- Doerfert, J., Träbert, E., Wolf, A., Schwalm, D., & Uwira, O. 1997, PhRvL, 78, 4355
- Ekman, J., Jönsson, P., Gustafsson, S., et al. 2014, A&A, 564, A24
- Engström, L., Denne, B., Ekberg, J. O., et al. 1981, PhysS, 24, 551
- Feldman, U., Behring, W. E., Curdt, W., et al. 1997, ApJS, 113, 195
- Fernández-Menchero, L., Del Zanna, G., & Badnell, N. R. 2014, A&A, 566, A104
- Fernández-Menchero, L., Zatsarinny, O., & Bartschat, K. 2017, JPhB, 50, 065203
- Froese Fischer, C., Godefroid, M., Brage, T., Jönsson, P., & Gaigalas, G. 2016, JPhB, 49, 182004
- Froese Fischer, C., & Tachiev, G. 2004, ADNDT, 87, 1
- Gaigalas, G., Froese Fischer, C., Rynkun, P., & Jönsson, P. 2017, Atoms, 5, 6
- Gaigalas, G., Zalandauskas, T., & Fritzsch, S. 2004, CoPhC, 157, 239
- Gálvez, F. J., Buendía, E., & Sarsa, A. 2003, JChPh, 118, 6858
- Grant, I., McKenzie, B., Norrington, P., Mayers, D., & Pyper, N. 1980, CoPhC, 21, 207
- Grant, I. P. 2007, Relativistic Quantum Theory of Atoms and Molecules, doi:10.1007/978-0-387-35069-1
- Gu, M. F. 2005a, ADNDT, 89, 267
- . 2005b, ApJS, 156, 105
- . 2007, ApJS, 169, 154
- . 2008, CaJPh, 86, 675
- Ho, H. C., Johnson, W. R., Blundell, S. A., & Safranova, M. S. 2006, PhRvA, 74, 022510
- Irwin, D. J. G., Livingston, A. E., & Kernahan, J. A. 1973, CaJPh, 51, 1948
- Jönsson, P., Froese Fischer, C., & Träbert, E. 1998, JPhB, 31, 3497
- Jönsson, P., Gaigalas, G., Bieroń, J., Froese Fischer, C., & Grant, I. P. 2013, CoPhC, 184, 2197
- Jönsson, P., He, X., Froese Fischer, C., & Grant, I. 2007, CaJPh, 177, 597
- Jönsson, P., Ekman, J., Gustafsson, S., et al. 2013, A&A, 559, p. A100
- Kallman, T. R., & Palmeri, P. 2007, RvMP, 79, 79
- Knystautas, E., Buchet-Poulizac, M. C., Buchet, J. P., & Druetta, M. 1979, J. Opt. Soc. Am., 69, 474
- Ko, Y. K., Raymond, J. C., Li, J., et al. 2002, ApJ, 578, 979
- Komasa, J., Rychlewski, J., & Jankowski, K. 2002, PhRvA, 65, 042507
- Kramida, A., Ralchenko, Y., Reader, J., & and NIST ASD Team. 2016, NIST Atomic Spectra Database (ver. 5.4), [Online]. Available: <http://physics.nist.gov/asd>
- National Institute of Standards and Technology, Gaithersburg, MD., ,
- Kunze, H.-J. 1972, SSRv, 13, 565
- Landi, E., & Young, P. R. 2009, ApJ, 706, 1
- Li, J., Jönsson, P., Dong, C., & Gaigalas, G. 2010, JPhB, 43, 035005
- Lindgren, I. 1974, JPhB, 7, 2441
- Marques, J. P., Parente, F., Costa, A. M., et al. 2012, PhRvA, 86, 052521
- Olsen, J., Roos, B. O., Jørgensen, P., & Jensen, H. J. A. 1988, J. Chem. Phys., 89, 2185
- Parenti, S., Vial, J.-C., & Lemaire, P. 2005, A&A, 443, 679
- Pehlivan Rhodin, A., Hartman, H., Nilsson, H., & Jönsson, P. 2017, A&A, 598, A102
- Penston, M. V., & Lago, M. T. V. T. 1983, MNRAS, 202, 77
- Raassen, A. J. J., & Pollock, A. M. T. 2013, A&A, 550, A55
- Raassen, A. J. J., Mewe, R., Audard, M., et al. 2002, A&A, 389, 228
- Radžić, L., Ekman, J., Jönsson, P., & Gaigalas, G. 2015, A&A, 582, A61
- Reistad, N., Hutton, R., Nilsson, A. E., Martinson, I., & Mannervik, S. 1986, PhysS, 34, 151
- Rubin, R. H., Ferland, G. J., Chollet, E. E., & Horstmeier, R. 2004, ApJ, 605, 784
- Ruffoni, M. P., Allende Prieto, C., Nave, G., & Pickering, J. C. 2013, ApJ, 779, 17
- Safranova, M. S., Johnson, W. R., & Safranova, U. I. 1996, PhRvA, 53, 4036
- . 1997, JPhB, 30, 2375

- Safronova, U. I., Derevianko, A., Safronova, M. S., & Johnson, W. R. 1999, JPhB, 32, 3527
- Sakho, I., Diop, B., Faye, M., et al. 2013, ADNDT, 99, 447
- Savukov, I. M., & Markhotok, A. A. 2006, JPhB, 39, 2115
- Si, R., Li, S., Guo, X. L., et al. 2016, ApJS, 227, 16
- Sturesson, L., Jönsson, P., & Froese Fischer, C. 2007, CoPhC, 177, 539
- Tachiev, G., & Froese Fischer, C. 1999, JPhB, 32, 5805
- Thomas, R. J., & Neupert, W. M. 1994, ApJS, 91, 461
- Tian, H., Curdt, W., Teriaca, L., Landi, E., & Marsch, E. 2009, A&A, 505, 307
- Träbert, E., Beiersdorfer, P., Brickhouse, N. S., & Golub, L. 2014a, ApJS, 215, 6
- . 2014b, ApJS, 211, 14
- Träbert, E., Knystautas, E. J., Saathoff, G., & Wolf, A. 2005, JPhB, 38, 2395
- Träbert, E., Wolf, A., Linkemann, J., & Tordoir, X. 1999, JPhB, 32, 537
- Verdebout, S., Nazé, C., Jönsson, P., et al. 2014, ADNDT, 100, 1111
- Vilkas, M. J., Ishikawa, Y., & Koc, K. 1999, PhRvA, 60, 2808
- Wang, K., Chen, Z. B., Chen, C. Y., et al. 2017a, ADNDT, 117-118, 174
- Wang, K., & Jönsson, P. 2017, in progress
- Wang, K., Yang, X., Chen, Z. B., et al. 2017b, ADNDT, 117-118, 1
- Wang, K., Li, D. F., Liu, H. T., et al. 2014, ApJS, 215, 26
- Wang, K., Guo, X. L., Liu, H. T., et al. 2015, ApJS, 218, 16
- Wang, K., Si, R., Dang, W., et al. 2016a, ApJS, 223, 3
- Wang, K., Chen, Z. B., Si, R., et al. 2016b, ApJS, 226, 14
- Wang, K., Jönsson, P., Ekman, J., et al. 2017c, ApJS, 229, 37
- Werner, K., Rauch, T., Reiff, E., Kruk, J. W., & Napiwotzki, R. 2004, A&A, 427, 685
- Zatsarinny, O., & Froese Fischer, C. 2009, CoPhC, 180, 2041
- Zhang, M., & Gou, B. C. 2005, Int. J Mod. Phys. C, 16, 951

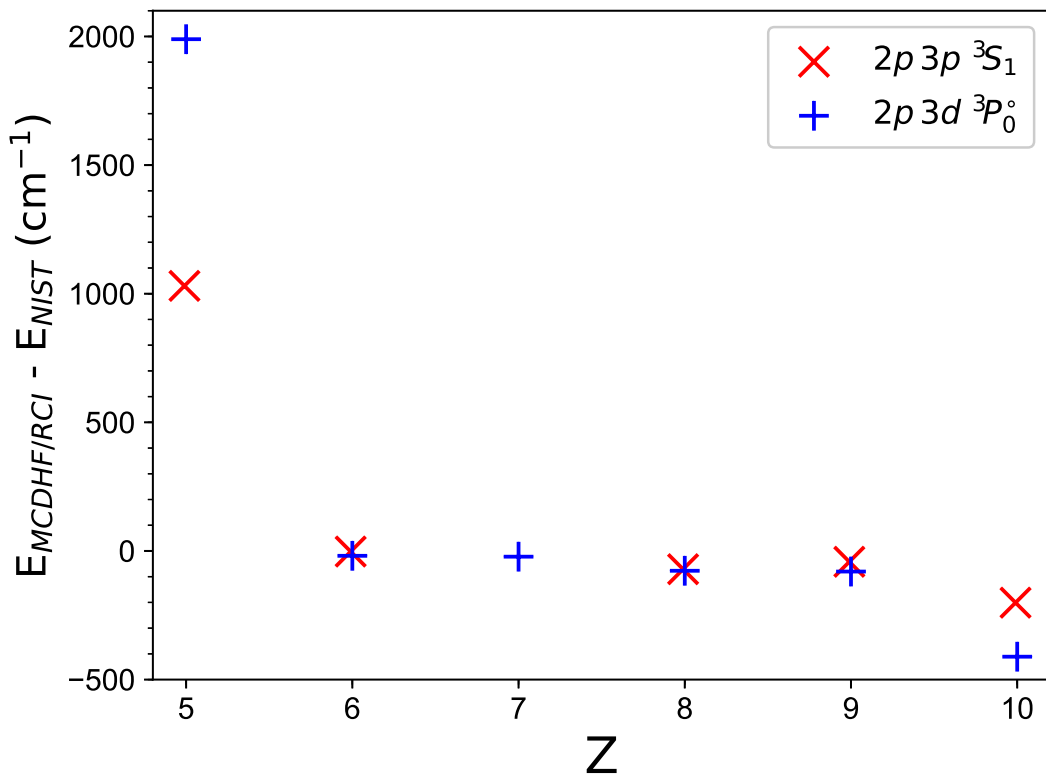


**Figure 1.** Energy differences in  $\text{cm}^{-1}$  of the MCDHF/RCI and NIST excitation energies as a function of  $Z$  for the  $2p3p\ ^3S_1$  and  $2p3d\ ^3P_0^\circ$  levels. The data come from Table 4.

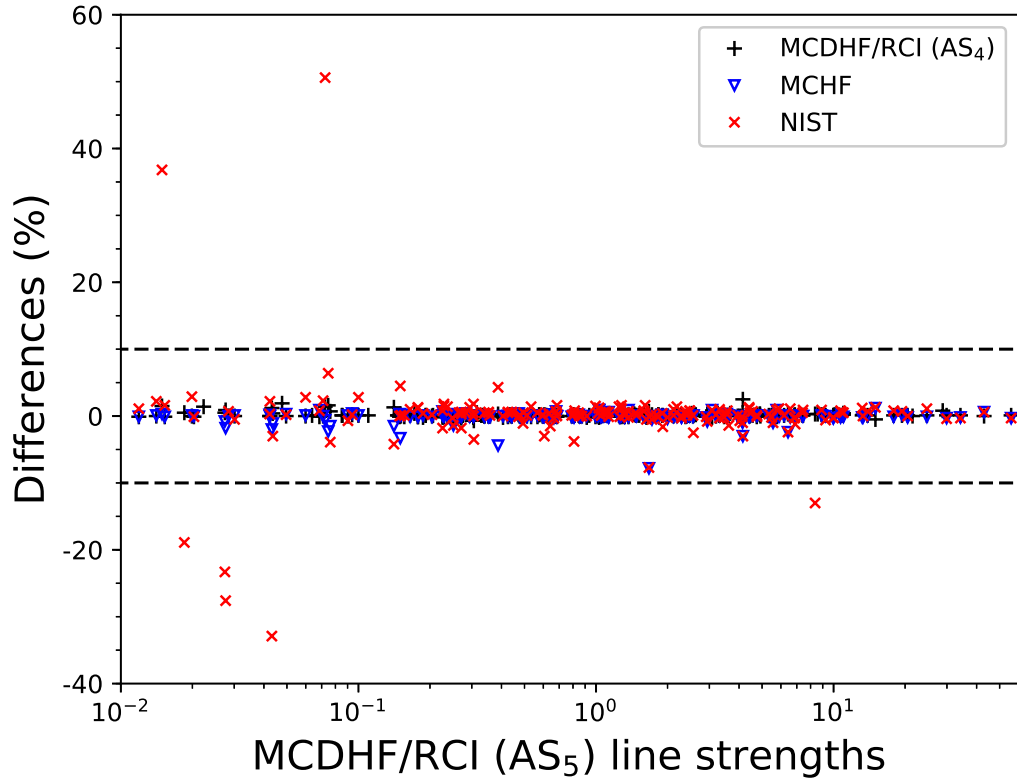


**Figure 2.** The differences ( $S_{\text{other}}/S_{\text{MCDHF/RCI(AS}_5)} - 1$ ) in % of line strengths  $S$  (in length form) for the transitions among the lowest 20 levels up to the  $2s3d$  configuration for the ions from B II to Ne VII from different resources, MCDHF/RCI (AS<sub>4</sub>), MCHF/BP, and NIST, relative to the values of the present MCDHF/RCI (AS<sub>5</sub>) calculations.

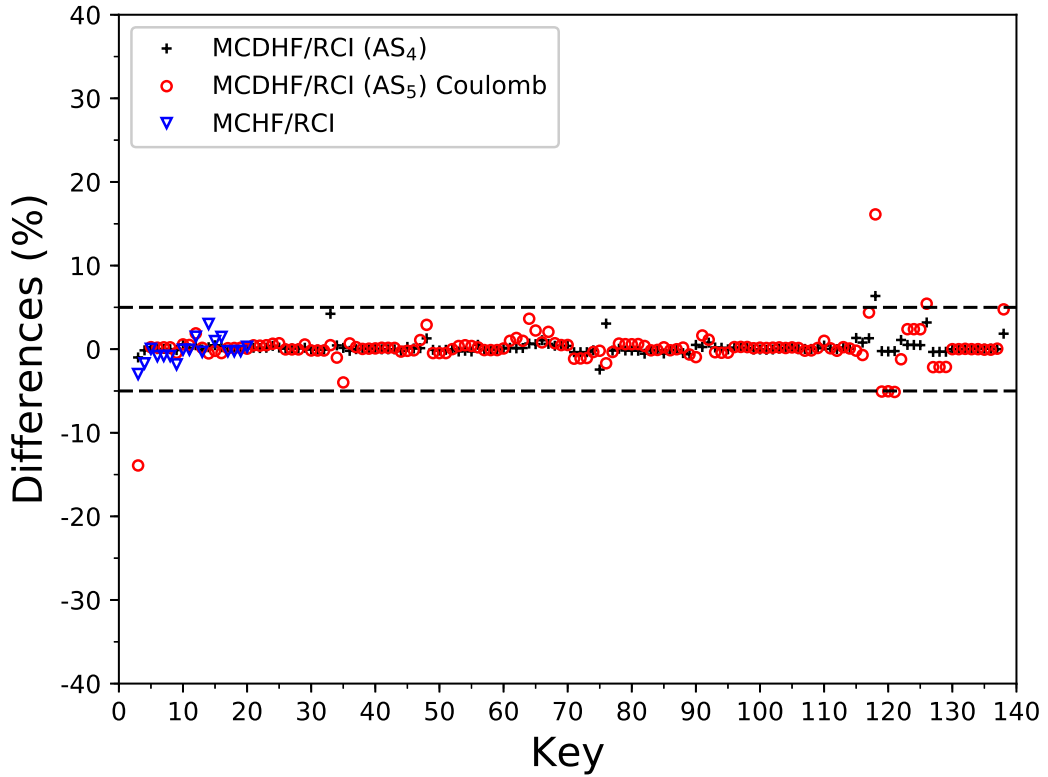


**Figure 3.** The differences ( $\tau_{\text{other}}/\tau_{\text{MCDHF/RCI(AS}_5)} - 1$ ) in % of lifetimes  $\tau$  for all the 138 levels in Ne VII from different resources, MCDHF/RCI (AS<sub>4</sub>) in Babushkin gauge, MCDHF/RCI (AS<sub>5</sub>) in Coulomb gauge, and MCHF/BP, relative to the values of the present MCDHF/RCI (AS<sub>5</sub>) calculations in Babushkin gauge.

**Table 1.** Excitation energies (in  $\text{cm}^{-1}$ ) and lifetimes ( $\tau$  in s) for all the levels of Be-like ions with  $Z = 5 - 10$  from the present MCDHF/RCI calculations. The total angular momentum and parity  $J^\pi$  are also included in column 4. The rightmost column gives the  $LS$  coupling expansion coefficients of the levels, in which the first number is the expansion coefficient for the leading  $LS$ -composition.

$Z$	Key	Level	$J^\pi$	$E_{\text{MCDHF/RCI}}$	$\tau_{\text{MCDHF/RCI}}$	$LS$ -composition
10	1	$2s^2 \ ^1S_0$	$0^e$	0	0.000E+00	$0.94 + 0.06 \ 2p^2 \ ^1S$
10	2	$2s2p \ ^3P_0^\circ$	$0^o$	111197	0.000E+00	1.00
10	3	$2s2p \ ^3P_1^\circ$	$1^o$	111649	5.277E-05	1.00
10	4	$2s2p \ ^3P_2^\circ$	$2^o$	112643	1.419E+01	1.00
10	5	$2s2p \ ^1P_1^\circ$	$1^o$	215065	2.508E-10	0.99
10	6	$2p^2 \ ^3P_0$	$0^e$	289259	3.249E-10	0.99
10	7	$2p^2 \ ^3P_1$	$1^e$	289771	3.235E-10	0.99
10	8	$2p^2 \ ^3P_2$	$2^e$	290653	3.213E-10	0.99
10	9	$2p^2 \ ^1D_2$	$2^e$	317716	1.811E-09	0.99
10	10	$2p^2 \ ^1S_0$	$0^e$	393321	1.769E-10	$0.92 + 0.06 \ 2s^2 \ ^1S$
10	11	$2s3s \ ^3S_1$	$1^e$	978197	1.788E-11	$0.97 + 0.02 \ 2p3p \ ^3S$
10	12	$2s3s \ ^1S_0$	$0^e$	998117	5.560E-11	$0.96 + 0.04 \ 2p3p \ ^1S$
10	13	$2s3p \ ^1P_1^\circ$	$1^o$	1025546	8.302E-12	$0.90 + 0.08 \ 2p3s \ ^1P^\circ$
10	14	$2s3p \ ^3P_0^\circ$	$0^o$	1028265	1.758E-09	0.98
10	15	$2s3p \ ^3P_1^\circ$	$1^o$	1028397	9.983E-10	0.98
10	16	$2s3p \ ^3P_2^\circ$	$2^o$	1028650	1.710E-09	0.98
10	17	$2s3d \ ^3D_1$	$1^e$	1054223	4.144E-12	0.98
10	18	$2s3d \ ^3D_2$	$2^e$	1054264	4.149E-12	0.98
10	19	$2s3d \ ^3D_3$	$3^e$	1054337	4.157E-12	0.98
10	20	$2s3d \ ^1D_2$	$2^e$	1071866	6.468E-12	0.98
10	21	$2p3s \ ^3P_0^\circ$	$0^o$	1119967	2.374E-11	0.98
10	22	$2p3s \ ^3P_1^\circ$	$1^o$	1120462	2.365E-11	0.98
10	23	$2p3s \ ^3P_2^\circ$	$2^o$	1121548	2.348E-11	0.98
10	24	$2p3s \ ^1P_1^\circ$	$1^o$	1138711	2.016E-11	$0.90 + 0.08 \ 2s3p \ ^1P^\circ$
10	25	$2p3p \ ^1P_1$	$1^e$	1148548	1.547E-11	0.99
10	26	$2p3p \ ^3D_1$	$1^e$	1154407	3.165E-11	0.97
10	27	$2p3p \ ^3D_2$	$2^e$	1154989	3.192E-11	0.98
10	28	$2p3p \ ^3D_3$	$3^e$	1155998	3.180E-11	0.98
10	29	$2p3p \ ^3S_1$	$1^e$	1165319	1.790E-11	$0.96 + 0.02 \ 2s3s \ ^3S$
10	30	$2p3p \ ^3P_0$	$0^e$	1171685	1.827E-11	0.99
10	31	$2p3p \ ^3P_1$	$1^e$	1172082	1.827E-11	0.99
10	32	$2p3p \ ^3P_2$	$2^e$	1172665	1.829E-11	0.99
10	33	$2p3d \ ^3F_2^\circ$	$2^o$	1177587	1.542E-10	$0.93 + 0.06 \ 2p3d \ ^1D^\circ$
10	34	$2p3d \ ^3F_3^\circ$	$3^o$	1178262	1.990E-09	0.99
10	35	$2p3d \ ^3F_4^\circ$	$4^o$	1179037	7.291E-09	0.99
10	36	$2p3d \ ^1D_2^\circ$	$2^o$	1179839	1.013E-11	$0.94 + 0.06 \ 2p3d \ ^3F^\circ$
10	37	$2p3p \ ^1D_2$	$2^e$	1184428	1.249E-11	0.98
10	38	$2p3d \ ^3D_1^\circ$	$1^o$	1193771	3.455E-12	0.99
10	39	$2p3d \ ^3D_2^\circ$	$2^o$	1193989	3.467E-12	0.99
10	40	$2p3d \ ^3D_3^\circ$	$3^o$	1194354	3.450E-12	1.00
10	41	$2p3d \ ^3P_2^\circ$	$2^o$	1199678	6.441E-12	0.96
10	42	$2p3d \ ^3P_1^\circ$	$1^o$	1200102	6.450E-12	0.96

*Table 1 continued*

**Table 1** (*continued*)

<i>Z</i>	Key	Level	<i>J</i> <sup>π</sup>	<i>E</i> <sub>MCDHF/RCI</sub>	<i>τ</i> <sub>MCDHF/RCI</sub>	<i>LS</i> -composition
10	43	$2p3d\ ^3P_0^o$	$0^o$	1200339	6.472E-12	0.97
10	44	$2p3p\ ^1S_0$	$0^e$	1205819	2.755E-11	$0.92 + 0.04\ 2s3s\ ^1S + 0.02\ 2s4s\ ^1S$
10	45	$2p3d\ ^1F_3^o$	$3^o$	1212072	3.000E-12	0.97
10	46	$2p3d\ ^1P_1^o$	$1^o$	1218082	5.155E-12	0.98
10	47	$2s4s\ ^3S_1$	$1^e$	1298906	4.119E-11	0.99
10	48	$2s4s\ ^1S_0$	$0^e$	1306994	4.656E-11	0.96
10	49	$2s4p\ ^3P_0^o$	$0^o$	1317970	1.274E-10	0.99
10	50	$2s4p\ ^3P_1^o$	$1^o$	1318016	1.259E-10	0.99
10	51	$2s4p\ ^3P_2^o$	$2^o$	1318126	1.283E-10	0.99
10	52	$2s4p\ ^1P_1^o$	$1^o$	1319731	1.633E-11	0.97
10	53	$2s4d\ ^3D_1$	$1^e$	1328043	1.056E-11	1.00
10	54	$2s4d\ ^3D_2$	$2^e$	1328057	1.057E-11	1.00
10	55	$2s4d\ ^3D_3$	$3^e$	1328082	1.058E-11	1.00
10	56	$2s4d\ ^1D_2$	$2^e$	1333874	1.356E-11	0.99
10	57	$2s4f\ ^3F_2^o$	$2^o$	1335111	2.730E-11	0.99
10	58	$2s4f\ ^3F_3^o$	$3^o$	1335119	2.730E-11	0.99
10	59	$2s4f\ ^3F_4^o$	$4^o$	1335132	2.730E-11	0.99
10	60	$2s4f\ ^1F_3^o$	$3^o$	1336905	2.652E-11	0.98
10	61	$2p4s\ ^3P_0^o$	$0^o$	1430746	4.405E-11	0.99
10	62	$2p4s\ ^3P_1^o$	$1^o$	1431042	4.180E-11	$0.89 + 0.09\ 2p4s\ ^1P^o$
10	63	$2p4s\ ^3P_2^o$	$2^o$	1432355	4.336E-11	0.99
10	64	$2p4s\ ^1P_1^o$	$1^o$	1433369	2.986E-11	$0.74 + 0.15\ 2s5p\ ^1P^o + 0.10\ 2p4s\ ^3P^o$
10	65	$2s5s\ ^3S_1$	$1^e$	1436099	3.333E-11	$0.85 + 0.14\ 2p4p\ ^3S$
10	66	$2s5s\ ^1S_0$	$0^e$	1438826	1.136E-10	$0.89 + 0.10\ 2p4p\ ^1S$
10	67	$2p4p\ ^1P_1$	$1^e$	1443735	2.718E-11	$0.86 + 0.13\ 2p4p\ ^3D$
10	68	$2p4p\ ^3D_1$	$1^e$	1445277	2.697E-11	$0.84 + 0.13\ 2p4p\ ^1P$
10	69	$2p4p\ ^3D_2$	$2^e$	1445610	2.669E-11	$0.97 + 0.02\ 2s5d\ ^3D$
10	70	$2p4p\ ^3D_3$	$3^e$	1446554	2.583E-11	$0.97 + 0.03\ 2s5d\ ^3D$
10	71	$2s5p\ ^3P_0^o$	$0^o$	1446973	9.947E-11	$0.94 + 0.05\ 2p4d\ ^3P^o$
10	72	$2s5p\ ^3P_1^o$	$1^o$	1446984	9.799E-11	$0.94 + 0.06\ 2p4d\ ^3P^o$
10	73	$2s5p\ ^3P_2^o$	$2^o$	1447007	9.524E-11	$0.94 + 0.06\ 2p4d\ ^3P^o$
10	74	$2s5p\ ^1P_1^o$	$1^o$	1450833	3.157E-11	$0.81 + 0.16\ 2p4s\ ^1P^o + 0.03\ 2p4d\ ^1P^o$
10	75	$2p4p\ ^3P_0$	$0^e$	1450874	2.948E-11	0.99
10	76	$2p4p\ ^3P_1$	$1^e$	1450992	3.201E-11	$0.79 + 0.17\ 2p4p\ ^3S + 0.03\ 2s5s\ ^3S$
10	77	$2p4p\ ^3P_2$	$2^e$	1451781	2.927E-11	0.98
10	78	$2p4p\ ^3S_1$	$1^e$	1452229	4.105E-11	$0.68 + 0.21\ 2p4p\ ^3P + 0.11\ 2s5s\ ^3S$
10	79	$2s5d\ ^3D_1$	$1^e$	1452978	2.490E-11	0.98
10	80	$2s5d\ ^3D_2$	$2^e$	1452995	2.532E-11	$0.97 + 0.02\ 2p4p\ ^3D$
10	81	$2p4d\ ^3F_2^o$	$2^o$	1453024	5.486E-11	$0.60 + 0.37\ 2s5f\ ^3F^o + 0.02\ 2p4d\ ^1D^o$
10	82	$2s5d\ ^3D_3$	$3^e$	1453025	2.602E-11	$0.97 + 0.03\ 2p4p\ ^3D$
10	83	$2s5g\ ^3G_3$	$3^e$	1453199	6.466E-11	$0.75 + 0.24\ 2p4f\ ^3G$
10	84	$2s5g\ ^3G_4$	$4^e$	1453257	6.656E-11	$0.58 + 0.18\ 2s5g\ ^1G + 0.18\ 2p4f\ ^3G$
10	85	$2p4d\ ^3F_3^o$	$3^o$	1453375	5.527E-11	$0.55 + 0.43\ 2s5f\ ^3F^o$
10	86	$2s5g\ ^3G_5$	$5^e$	1453496	6.837E-11	$0.79 + 0.21\ 2p4f\ ^3G$
10	87	$2s5g\ ^1G_4$	$4^e$	1453566	7.312E-11	$0.61 + 0.19\ 2s5g\ ^3G + 0.15\ 2p4f\ ^1G$
10	88	$2s5f\ ^3F_4^o$	$4^o$	1453809	5.744E-11	$0.53 + 0.47\ 2p4d\ ^3F^o$
10	89	$2s5f\ ^1F_3^o$	$3^o$	1454855	3.425E-11	$0.86 + 0.12\ 2p4d\ ^1F^o$
10	90	$2s5d\ ^1D_2$	$2^e$	1454971	8.321E-11	$0.62 + 0.37\ 2p4p\ ^1D$
10	91	$2p4d\ ^1D_2^o$	$2^o$	1455742	1.957E-11	$0.95 + 0.04\ 2s5f\ ^3F^o$
10	92	$2p4p\ ^1D_2$	$2^e$	1456542	1.456E-11	$0.60 + 0.38\ 2s5d\ ^1D$

*Table 1 continued*

**Table 1** (*continued*)

<i>Z</i>	Key	Level	<i>J</i> <sup>π</sup>	<i>E</i> <sub>MCDHF/RCI</sub>	<i>τ</i> <sub>MCDHF/RCI</sub>	<i>LS</i> -composition
10	93	$2s5f\ ^3F_2^o$	$2^o$	1457897	4.559E-11	$0.58 + 0.38\ 2p4d\ ^3F^o$
10	94	$2s5f\ ^3F_3^o$	$3^o$	1458067	4.667E-11	$0.55 + 0.43\ 2p4d\ ^3F^o$
10	95	$2p4d\ ^3F_4^o$	$4^o$	1458479	5.025E-11	$0.52 + 0.47\ 2s5f\ ^3F^o$
10	96	$2p4d\ ^3D_1^o$	$1^o$	1460317	8.417E-12	$0.97 + 0.02\ 2p4d\ ^3P^o$
10	97	$2p4d\ ^3D_2^o$	$2^o$	1460552	8.648E-12	$0.93 + 0.05\ 2p4d\ ^3P^o$
10	98	$2p4d\ ^3D_3^o$	$3^o$	1460970	8.447E-12	0.98
10	99	$2p4f\ ^1F_3$	$3^e$	1461766	2.734E-11	$0.68 + 0.28\ 2p4f\ ^3F + 0.03\ 2p4f\ ^3D$
10	100	$2p4f\ ^3F_2$	$2^e$	1461890	2.823E-11	0.97
10	101	$2p4f\ ^3F_3$	$3^e$	1462168	2.801E-11	$0.68 + 0.29\ 2p4f\ ^1F$
10	102	$2p4f\ ^3F_4$	$4^e$	1462286	2.844E-11	0.98
10	103	$2p4d\ ^3P_2^o$	$2^o$	1463091	1.423E-11	$0.87 + 0.05\ 2p4d\ ^3D^o + 0.05\ 2s5p\ ^3P^o$
10	104	$2p4d\ ^3P_1^o$	$1^o$	1463451	1.444E-11	$0.91 + 0.05\ 2s5p\ ^3P^o + 0.02\ 2p4d\ ^3D^o$
10	105	$2p4d\ ^3P_0^o$	$0^o$	1463646	1.466E-11	$0.93 + 0.05\ 2s5p\ ^3P^o$
10	106	$2p4f\ ^3D_3$	$3^e$	1466327	2.865E-11	0.96
10	107	$2p4f\ ^3G_3$	$3^e$	1466383	3.283E-11	$0.74 + 0.23\ 2s5g\ ^3G$
10	108	$2p4p\ ^1S_0$	$0^e$	1466386	3.720E-11	$0.85 + 0.09\ 2s5s\ ^1S$
10	109	$2p4f\ ^3G_4$	$4^e$	1466595	3.349E-11	$0.64 + 0.20\ 2s5g\ ^3G + 0.11\ 2p4f\ ^1G$
10	110	$2p4f\ ^3D_2$	$2^e$	1466598	2.884E-11	$0.80 + 0.16\ 2p4f\ ^1D + 0.02\ 2p4f\ ^3F$
10	111	$2p4f\ ^3D_1$	$1^e$	1467077	2.866E-11	0.99
10	112	$2p4f\ ^3G_5$	$5^e$	1467252	3.225E-11	$0.78 + 0.21\ 2s5g\ ^3G$
10	113	$2p4f\ ^1D_2$	$2^e$	1467610	2.965E-11	$0.80 + 0.18\ 2p4f\ ^3D$
10	114	$2p4f\ ^1G_4$	$4^e$	1467806	3.740E-11	$0.68 + 0.17\ 2s5g\ ^1G + 0.12\ 2p4f\ ^3G$
10	115	$2p4d\ ^1F_3^o$	$3^o$	1469623	7.537E-12	$0.86 + 0.12\ 2s5f\ ^1F^o$
10	116	$2p4d\ ^1P_1^o$	$1^o$	1470147	1.158E-11	$0.95 + 0.03\ 2s5p\ ^1P^o$
10	117	$2s6s\ ^3S_1$	$1^e$	1512005	1.107E-10	0.99
10	118	$2s6s\ ^1S_0$	$0^e$	1514042	1.156E-10	0.98
10	119	$2s6p\ ^3P_0^o$	$0^o$	1517319	2.179E-10	1.00
10	120	$2s6p\ ^3P_1^o$	$1^o$	1517332	2.167E-10	0.99
10	121	$2s6p\ ^3P_2^o$	$2^o$	1517363	2.194E-10	1.00
10	122	$2s6p\ ^1P_1^o$	$1^o$	1517824	4.591E-11	0.98
10	123	$2s6d\ ^3D_1$	$1^e$	1520185	3.602E-11	1.00
10	124	$2s6d\ ^3D_2$	$2^e$	1520189	3.605E-11	1.00
10	125	$2s6d\ ^3D_3$	$3^e$	1520196	3.610E-11	1.00
10	126	$2s6d\ ^1D_2$	$2^e$	1521680	4.097E-11	1.00
10	127	$2s6f\ ^3F_2^o$	$2^o$	1521981	8.813E-11	1.00
10	128	$2s6f\ ^3F_3^o$	$3^o$	1521984	8.813E-11	1.00
10	129	$2s6f\ ^3F_4^o$	$4^o$	1521987	8.813E-11	1.00
10	130	$2s6h\ ^3H_4^o$	$4^o$	1522131	2.538E-10	1.00
10	131	$2s6h\ ^3H_5^o$	$5^o$	1522133	2.538E-10	$0.71 + 0.29\ 2s6h\ ^1H^o$
10	132	$2s6h\ ^1H_5^o$	$5^o$	1522134	2.539E-10	$0.71 + 0.29\ 2s6h\ ^3H^o$
10	133	$2s6h\ ^3H_6^o$	$6^o$	1522135	2.539E-10	1.00
10	134	$2s6g\ ^3G_3$	$3^e$	1522380	1.586E-10	0.99
10	135	$2s6g\ ^3G_4$	$4^e$	1522384	1.585E-10	0.99
10	136	$2s6g\ ^3G_5$	$5^e$	1522390	1.583E-10	0.99
10	137	$2s6g\ ^1G_4$	$4^e$	1522406	1.605E-10	0.99
10	138	$2s6f\ ^1F_3^o$	$3^o$	1522569	8.574E-11	0.99

NOTE— Table 1 is published in its entirety in the machine-readable format. The values for Ne vii are shown here for guidance regarding its form and content.

**Table 2.** The MCDHF/RCI excitation energies in  $\text{cm}^{-1}$  for Ne VII as a function of the increasing size of the CSF expansion. AS<sub>1</sub>, AS<sub>2</sub>, AS<sub>3</sub>, AS<sub>4</sub>, and AS<sub>5</sub> – the present MCDHF/RCI excitation energies; NIST – the compiled values from the NIST ASD (Kramida et al. 2016);  $\Delta E$  – the differences between the MCDHF/RCI calculated energies for AS<sub>5</sub> and the NIST compiled values.

Key	Level	MCDHF/RCI					NIST	$\Delta E$
		AS <sub>1</sub>	AS <sub>2</sub>	AS <sub>3</sub>	AS <sub>4</sub>	AS <sub>5</sub>		
1	$2s^2 \ ^1S_0$	0	0	0	0	0	0	...
2	$2s2p \ ^3P_0^o$	111669	111132	111139	111182	111197	111252.8	-55.8
3	$2s2p \ ^3P_1^o$	112120	111585	111591	111635	111649	111708	-59
4	$2s2p \ ^3P_2^o$	113113	112578	112585	112628	112643	112702.4	-59.4
5	$2s2p \ ^1P_1^o$	221483	216852	215442	215156	215065	214951.6	113.4
6	$2p^2 \ ^3P_0$	291107	289527	289213	289244	289259	289330.4	-71.4
7	$2p^2 \ ^3P_1$	291616	290038	289724	289756	289771	289841.1	-70.1
8	$2p^2 \ ^3P_2$	292492	290920	290606	290638	290653	290724	-71
9	$2p^2 \ ^1D_2$	323947	319602	318039	317795	317716	317694.6	21.4
10	$2p^2 \ ^1S_0$	403011	396937	394131	393548	393321	393125	196
11	$2s3s \ ^3S_1$	976595	977785	978086	978176	978197	978300.29	-103.29
12	$2s3s \ ^1S_0$	996817	997839	998072	998119	998117	998183.1	-66.1
13	$2s3p \ ^1P_1^o$	1024798	1025294	1025472	1025545	1025546	1025620.6	-74.6
14	$2s3p \ ^3P_0^o$	1027060	1027865	1028154	1028238	1028265	1028366.7	-101.7
15	$2s3p \ ^3P_1^o$	1027195	1027999	1028286	1028371	1028397	1028499.59	-102.59
16	$2s3p \ ^3P_2^o$	1027448	1028253	1028540	1028624	1028650	1028755.1	-105.1
17	$2s3d \ ^3D_1$	1053250	1053777	1054153	1054199	1054223	1054310	-87
18	$2s3d \ ^3D_2$	1053290	1053818	1054194	1054240	1054264	1054354.4	-90.4
19	$2s3d \ ^3D_3$	1053363	1053892	1054267	1054313	1054337	1054428.3	-91.3
20	$2s3d \ ^1D_2$	1072973	1071889	1072002	1071885	1071866	1071914	-48
21	$2p3s \ ^3P_0^o$	1118966	1119624	1119872	1119947	1119968	1120207	-239
22	$2p3s \ ^3P_1^o$	1119465	1120120	1120367	1120442	1120462	1120720	-258
23	$2p3s \ ^3P_2^o$	1120550	1121203	1121452	1121527	1121548	1121757	-209
24	$2p3s \ ^1P_1^o$	1139867	1139160	1138821	1138802	1138711	1138860	-149
25	$2p3p \ ^1P_1$	1147663	1148244	1148439	1148527	1148548	1148647	-99
26	$2p3p \ ^3D_1$	1153890	1154259	1154343	1154395	1154407	1154488	-81
27	$2p3p \ ^3D_2$	1154478	1154844	1154926	1154977	1154989	1155120	-131
28	$2p3p \ ^3D_3$	1155491	1155854	1155935	1155986	1155998	1156150	-152
29	$2p3p \ ^3S_1$	1164957	1165272	1165267	1165316	1165319	1165520	-201
30	$2p3p \ ^3P_0$	1171124	1171343	1171561	1171657	1171685	1171500	185
31	$2p3p \ ^3P_1$	1171519	1171739	1171958	1172054	1172082	1172020	62
32	$2p3p \ ^3P_2$	1172100	1172321	1172541	1172637	1172665	1172350	315
33	$2p3d \ ^3F_2^o$	1177348	1177395	1177545	1177570	1177587	1177910	-323
34	$2p3d \ ^3F_3^o$	1178098	1178083	1178224	1178246	1178262	1178270	-8
35	$2p3d \ ^3F_4^o$	1178875	1178859	1178999	1179021	1179037	1179188	-151
36	$2p3d \ ^1D_2^o$	1178924	1179490	1179743	1179812	1179839	1180070	-231
37	$2p3p \ ^1D_2$	1185678	1184801	1184454	1184448	1184428	1185130	-702
38	$2p3d \ ^3D_1^o$	1192935	1193380	1193663	1193744	1193771	1194060	-289
39	$2p3d \ ^3D_2^o$	1193154	1193598	1193881	1193962	1193989	1194320	-331
40	$2p3d \ ^3D_3^o$	1193517	1193961	1194246	1194326	1194354	1194538	-184
41	$2p3d \ ^3P_2^o$	1199328	1199519	1199643	1199684	1199678	1199920	-242
42	$2p3d \ ^3P_1^o$	1199759	1199945	1200067	1200108	1200103	1200470	-367
43	$2p3d \ ^3P_0^o$	1200000	1200183	1200304	1200345	1200339	1200750	-411

Table 2 continued

**Table 2** (*continued*)

Key	Level	MCDHF/RCI					NIST	$\Delta E$
		AS <sub>1</sub>	AS <sub>2</sub>	AS <sub>3</sub>	AS <sub>4</sub>	AS <sub>5</sub>		
44	$2p3p\ ^1S_0$	1208965	1207269	1206010	1205937	1205819	1206150	-331
45	$2p3d\ ^1F_3^\circ$	1214298	1212220	1212122	1212081	1212072	1212060	12
46	$2p3d\ ^1P_1^\circ$	1219976	1218713	1218276	1218135	1218082	1218430	-348
47	$2s4s\ ^3S_1$	1297126	1298445	1298812	1298905	1298906	1299170	-264
48	$2s4s\ ^1S_0$	1305867	1306917	1307014	1307052	1306994	1307080	-86
49	$2s4p\ ^3P_0^\circ$	1316270	1317444	1317841	1317943	1317970	...	...
50	$2s4p\ ^3P_1^\circ$	1316317	1317490	1317887	1317989	1318016	...	...
51	$2s4p\ ^3P_2^\circ$	1316427	1317600	1317997	1318099	1318126	1318110	16
52	$2s4p\ ^1P_1^\circ$	1318587	1319402	1319667	1319748	1319731	1319890	-159
53	$2s4d\ ^3D_1$	1326548	1327511	1327934	1328016	1328043	1328390	-347
54	$2s4d\ ^3D_2$	1326562	1327525	1327948	1328030	1328057	1328265	-208
55	$2s4d\ ^3D_3$	1326587	1327551	1327974	1328055	1328083	1328318	-235
56	$2s4d\ ^1D_2$	1333388	1333548	1333850	1333864	1333874	1333900	-26
57	$2s4f\ ^3F_2^\circ$	1333429	1334516	1334968	1335077	1335111	1335190	-79
58	$2s4f\ ^3F_3^\circ$	1333436	1334523	1334976	1335084	1335119	1335300	-181
59	$2s4f\ ^3F_4^\circ$	1333449	1334536	1334989	1335097	1335132	1335347	-215
60	$2s4f\ ^1F_3^\circ$	1335457	1336329	1336768	1336873	1336905	1337056	-151
61	$2p4s\ ^3P_0^\circ$	1429435	1430311	1430633	1430725	1430746	1430600	146
62	$2p4s\ ^3P_1^\circ$	1429767	1430635	1430945	1431034	1431042	1431010	32
63	$2p4s\ ^3P_2^\circ$	1431047	1431918	1432242	1432334	1432355	1431990	365
64	$2p4s\ ^1P_1^\circ$	1432331	1433183	1433392	1433458	1433369	1433330	39
65	$2s5s\ ^3S_1$	1434237	1435578	1435996	1436099	1436099	1436460	-361
66	$2s5s\ ^1S_0$	1437011	1438294	1438706	1438812	1438826	1439400	-574
67	$2p4p\ ^1P_1$	1442500	1443313	1443613	1443716	1443735	1443980	-245
68	$2p4p\ ^3D_1$	1444097	1444879	1445157	1445254	1445277	1445400	-123
69	$2p4p\ ^3D_2$	1444440	1445216	1445491	1445586	1445610	1445700	-90
70	$2p4p\ ^3D_3$	1445374	1446158	1446434	1446530	1446554	1446760	-206
71	$2s5p\ ^3P_0^\circ$	1445084	1446386	1446832	1446941	1446974	...	...
72	$2s5p\ ^3P_1^\circ$	1445095	1446396	1446842	1446952	1446984	...	...
73	$2s5p\ ^3P_2^\circ$	1445121	1446420	1446866	1446975	1447008	...	...
74	$2s5p\ ^1P_1^\circ$	1450236	1450794	1450882	1450939	1450833	1450500	333
75	$2p4p\ ^3P_0$	1449768	1450426	1450739	1450847	1450874	1450600	274
76	$2p4p\ ^3P_1$	1449904	1450584	1450874	1450978	1450992	1451130	-138
77	$2p4p\ ^3P_2$	1450665	1451329	1451644	1451752	1451781	1452180	-399
78	$2p4p\ ^3S_1$	1451232	1452000	1452177	1452264	1452229	1452590	-361
79	$2s5d\ ^3D_1$	1451273	1452393	1452845	1452943	1452978	1452900	78
80	$2s5d\ ^3D_2$	1451272	1452411	1452862	1452960	1452995	1453100	-105
81	$2p4d\ ^3F_2^\circ$	1451646	1452555	1452914	1452999	1453024	1452990	34
82	$2s5d\ ^3D_3$	1451304	1452442	1452892	1452990	1453025	1453200	-175
83	$2s5g\ ^3G_3$	1451337	1452571	1453041	1453157	1453199	1453680	-481
84	$2s5g\ ^3G_4$	1451389	1452627	1453098	1453214	1453257	1453300	-43
85	$2p4d\ ^3F_3^\circ$	1451938	1452887	1453260	1453349	1453375	1453710	-335
86	$2s5g\ ^3G_5$	1451600	1452863	1453336	1453453	1453496	1453710	-214
87	$2s5g\ ^1G_4$	1451666	1452931	1453407	1453524	1453566	...	...
88	$2s5f\ ^3F_4^\circ$	1452293	1453297	1453687	1453782	1453809	1454010	-201
89	$2s5f\ ^1F_3^\circ$	1453117	1454261	1454711	1454821	1454855	1454950	-95
90	$2s5d\ ^1D_2$	1454151	1454692	1454891	1454959	1454971	1455400	-429
91	$2p4d\ ^1D_2^\circ$	1454450	1455311	1455632	1455715	1455742	1455930	-188

Table 2 continued

**Table 2** (*continued*)

Key	Level	MCDHF/RCI					NIST	$\Delta E$
		AS <sub>1</sub>	AS <sub>2</sub>	AS <sub>3</sub>	AS <sub>4</sub>	AS <sub>5</sub>		
92	$2p4p\ ^1D_2$	1455985	1456324	1456507	1456554	1456542	1456680	-138
93	$2s5f\ ^3F_2^o$	1456615	1457419	1457787	1457868	1457897	1458260	-363
94	$2s5f\ ^3F_3^o$	1456825	1457600	1457961	1458040	1458067	1458419	-352
95	$2p4d\ ^3F_4^o$	1457319	1458038	1458380	1458453	1458479	1458703	-224
96	$2p4d\ ^3D_1^o$	1459119	1459877	1460201	1460291	1460317	1460600	-283
97	$2p4d\ ^3D_2^o$	1459357	1460114	1460438	1460527	1460552	1461110	-558
98	$2p4d\ ^3D_3^o$	1459767	1460523	1460851	1460940	1460970	1461220	-250
99	$2p4f\ ^1F_3$	1460340	1461229	1461618	1461728	1461766	1462080	-314
100	$2p4f\ ^3F_2$	1460464	1461353	1461744	1461852	1461890	1462080	-190
101	$2p4f\ ^3F_3$	1460736	1461628	1462020	1462130	1462168	1462830	-662
102	$2p4f\ ^3F_4$	1460852	1461745	1462138	1462248	1462286	1462550	-264
103	$2p4d\ ^3P_2^o$	1462152	1462828	1463068	1463139	1463091	1462930	161
104	$2p4d\ ^3P_1^o$	1462526	1463195	1463432	1463502	1463451	1463390	61
105	$2p4d\ ^3P_0^o$	1462728	1463394	1463629	1463699	1463646	1464180	-534
106	$2p4f\ ^3D_3$	1465025	1465831	1466200	1466295	1466327	1466640	-313
107	$2p4f\ ^3G_3$	1465178	1465850	1466243	1466348	1466383	1466670	-287
108	$2p4p\ ^1S_0$	1468480	1468000	1466854	1466800	1466386	...	...
109	$2p4f\ ^3G_4$	1465405	1466060	1466455	1466559	1466595	1466569	26
110	$2p4f\ ^3D_2$	1465327	1466111	1466477	1466568	1466598	1467230	-632
111	$2p4f\ ^3D_1$	1465782	1466583	1466951	1467046	1467077	...	...
112	$2p4f\ ^3G_5$	1466084	1466722	1467113	1467217	1467252	1467457	-205
113	$2p4f\ ^1D_2$	1466471	1467153	1467511	1467584	1467610	1467730	-120
114	$2p4f\ ^1G_4$	1466699	1467267	1467665	1467770	1467806	1467946	-140
115	$2p4d\ ^1F_3^o$	1470523	1469558	1469658	1469630	1469623	1469550	73
116	$2p4d\ ^1P_1^o$	1470536	1470438	1470310	1470234	1470148	1470080	68
117	$2s6s\ ^3S_1$	1510056	1511462	1511910	1512014	1512005	1512110	-105
118	$2s6s\ ^1S_0$	1512793	1513993	1514114	1514181	1514042	...	...
119	$2s6p\ ^3P_0^o$	1515361	1516724	1517185	1517295	1517319	...	...
120	$2s6p\ ^3P_1^o$	1515374	1516737	1517198	1517308	1517332	1517740	-408
121	$2s6p\ ^3P_2^o$	1515405	1516768	1517228	1517339	1517363	1517741	-378
122	$2s6p\ ^1P_1^o$	1516163	1517387	1517762	1517854	1517824	1518600	-776
123	$2s6d\ ^3D_1$	1518268	1519569	1520041	1520150	1520185	1520100	85
124	$2s6d\ ^3D_2$	1518273	1519573	1520045	1520154	1520189	1520360	-171
125	$2s6d\ ^3D_3$	1518280	1519580	1520052	1520161	1520196	1520460	-264
126	$2s6d\ ^1D_2$	1520207	1521180	1521583	1521662	1521680	1521860	-180
127	$2s6f\ ^3F_2^o$	1520073	1521353	1521830	1521944	1521981	1522402	-421
128	$2s6f\ ^3F_3^o$	1520075	1521356	1521832	1521946	1521984	...	...
129	$2s6f\ ^3F_4^o$	1520078	1521359	1521836	1521950	1521987	...	...
130	$2s6h\ ^3H_4^o$	1520079	1521482	1521973	1522092	1522132	...	...
131	$2s6h\ ^3H_5^o$	1520079	1521483	1521974	1522093	1522133	1522421	-288
132	$2s6h\ ^1H_5^o$	1520080	1521485	1521975	1522094	1522134	1522420	-286
133	$2s6h\ ^3H_6^o$	1520081	1521486	1521976	1522095	1522135	...	...
134	$2s6g\ ^3G_3$	1520304	1521725	1522218	1522336	1522380	...	...
135	$2s6g\ ^3G_4$	1520308	1521729	1522222	1522340	1522384	...	...
136	$2s6g\ ^3G_5$	1520313	1521734	1522227	1522346	1522390	...	...
137	$2s6g\ ^1G_4$	1520331	1521750	1522243	1522362	1522406	...	...
138	$2s6f\ ^1F_3^o$	1520808	1521955	1522423	1522534	1522569	1523040	-471

**Table 3.** Computed excitation energies of Ne VII from the present MCDHF/RCI and MBPT calculations and from the calculations by Savukov & Markhotok (2006) [MBPT2], by Fernández-Menchero et al. (2014) [AUTOSTRUCTURE], by Safranova et al. (1996, 1997) [MBPT3], and by Tachiev & Froese Fischer (1999); Froese Fischer & Tachiev (2004) [MCHF/BP] are compared with the NIST compiled values.  $E$  – excitation energies from different resources ;  $\Delta E$  – the differences between the calculated energies from different resources and the NIST compiled values.

Key	Level	NIST		MCDHF/RCI		MBPT		MBPT2		AUTOSTRUCTURE		MBPT3		MCHF/BP		
		$E$	$E$	$E$	$\Delta E$	$E$	$\Delta E$	$E$	$\Delta E$	$E$	$\Delta E$	$E$	$\Delta E$	$E$	$\Delta E$	
1	$2s^2 \ 1S_0$	0	0	...	0	...	0	...	0	...	0	...	0	...	0	...
2	$2s2p \ 3P_0^o$	111252.8	111197	-55.8	111182	-70.8	111264	11.2	111924	671.2	111128	-124.8	111441	188.2		
3	$2s2p \ 3P_1^o$	111708	111649	-59	111592	-116	111708	0	112461	753	111582	-126	111896	188		
4	$2s2p \ 3P_2^o$	112702.4	112643	-59.4	112640	-62.4	112706	3.6	113551	848.6	112578	-124.4	112893	190.6		
5	$2s2p \ 1P_1^o$	214951.6	215065	113.4	214844	-107.6	215524	572.4	222371	7419.4	213581	-1370.6	215260	308.4		
6	$2p^2 \ 3P_0$	289330.4	289259	-71.4	289073	-257.4	289683	352.6	293008	3677.6	289144	-186.4	290029	698.6		
7	$2p^2 \ 3P_1$	289841.1	289771	-70.1	289606	-235.1	290190	348.9	293562	3720.9	289657	-184.1	290546	704.9		
8	$2p^2 \ 3P_2$	290724	290653	-71	290466	-258	291064	340	294617	3893	290544	-180	291429	705		
9	$2p^2 \ 1D_2$	317694.6	317716	21.4	317427	-267.6	318226	531.4	325887	8192.4	316463	-1231.6	318503	808.4		
10	$2p^2 \ 1S_0$	393125	393321	196	392529	-596	395227	2102	406762	13637	391881	-1244	394062	937		
11	$2s3s \ 3S_1$	978300.29	978197	-103.29	978452	151.71	978164	-136.29	974357	-3943.29	978538	237.71	978750	449.71		
12	$2s3s \ 1S_0$	998183.1	998117	-66.1	998253	69.9	998136	-47.1	994886	-3297.1	998633	449.9	998691	507.9		
13	$2s3p \ 1P_0^o$	1025620.6	1025546	-74.6	1025626	5.4	1025567	-53.6	1022913	-2707.6	1025607	-13.6	1026055	434.4		
14	$2s3p \ 3P_0^o$	1028366.7	1028265	-101.7	1028414	47.3	1028269	-97.7	1025090	-3276.7	1028665	165.41	1028884	384.41		
15	$2s3p \ 3P_1^o$	1028499.59	1028397	-102.59	1028529	29.41	1028401	-98.59	1025230	-3269.59	1028665	165.41	1028884	384.41		
16	$2s3p \ 3P_2^o$	1028755.1	1028650	-105.1	1028803	47.9	1028655	-100.1	1025476	-3279.1	1029139	383.9				
17	$2s3d \ 3D_1$	1054310	1054223	-87	1054414	104	1054207	-103	1051165	-3145	1054715	405				
18	$2s3d \ 3D_2$	1054354.4	1054264	-90.4	1054442	87.6	1054247	-107.4	1051221	-3133.4	1054380	25.6	1054755	400.6		
19	$2s3d \ 3D_3$	1054428.3	1054337	-91.3	1054523	94.7	1054320	-108.3	1051306	-3122.3	1054828	399.7				
20	$2s3d \ 1D_2$	1071914	1071866	-48	1071577	-337	1072003	89	1071133	-781	1071447	-467	1072321	407		
21	$2p3s \ 3P_0^o$	1120207	1119967	-240	1120118	-89	1120106	-101	1117750	-2457	1120697	-23				
22	$2p3s \ 3P_1^o$	1120720	1120462	-258	1120598	-122	1120596	-124	1118269	-2451	1120697	-23				
23	$2p3s \ 3P_2^o$	1121757	1121548	-209	1121705	-52	1121682	-75	1119381	-2376	1120697	-23				
24	$2p3s \ 1P_1^o$	1138860	1138711	-149	1138413	-447	1138883	23	1139450	590	1138115	-745	1138838	-292		
25	$2p3p \ 1P_1$	1148647	1148548	-99	1148767	120	1148735	88	1146126	-2521	1148824	177	1148824	177		
26	$2p3p \ 3D_1$	1154488	1154407	-81	1154595	107	1154577	89	1152534	-1954	1155162	42	1155162	42		
27	$2p3p \ 3D_2$	1155120	1154989	-131	1155165	45	1155157	37	1153130	-1990	1155162	42	1155162	42		
28	$2p3p \ 3D_3$	1156150	1155998	-152	1156185	35	1156162	12	1154145	-2005	1155162	42	1155162	42		
29	$2p3p \ 3S_1$	1165520	1165319	-201	1165476	-44	1165537	17	1163337	-2183	1165482	-38	1165482	-38		
30	$2p3p \ 3P_0$	1171500	1171685	185	1171576	76	1171907	407	1170262	-1238	1172349	329	1172349	329		
31	$2p3p \ 3P_1$	1172020	1172082	62	1171991	-29	1172304	284	1170671	-1349	1172349	329	1172349	329		
32	$2p3p \ 3P_2$	1172350	1172665	315	1172573	223	1172883	533	1171318	-1032	1172349	329	1172349	329		
33	$2p3d \ 3F_2^o$	1177910	1177587	-323	1177720	-190	1177740	-170	1175903	-2007	1172349	329	1172349	329		
34	$2p3d \ 3F_3^o$	1178270	1178262	-8	1178370	100	1178410	140	1176718	-1552	1178542	272	1178542	272		
35	$2p3d \ 3F_4^o$	1179188	1179037	-151	1179170	-18	1179181	-7	1177541	-1647	1178542	272	1178542	272		
36	$2p3d \ 1D_2^o$	1180070	1179839	-231	1180050	-20	1180017	-53	1177446	-2624	1180222	152	1180222	152		
37	$2p3p \ 1D_2$	1185130	1184428	-702	1184019	-1111	1184660	-470	1185441	311	1183838	-1292	1183838	-1292		
38	$2p3d \ 3D_1^o$	1194060	1193771	-289	1193946	-114	1194001	-59	1191457	-2603	1194276	-44	1194276	-44		
39	$2p3d \ 3D_2^o$	1194320	1193989	-331	1194167	-153	1194218	-102	1191682	-2638	1194276	-44	1194276	-44		
40	$2p3d \ 3D_3^o$	1194538	1194354	-184	1194521	-17	1194581	43	1192066	-2472	1194276	-44	1194276	-44		
41	$2p3d \ 3P_2^o$	1199920	1199678	-242	1199838	-82	1199942	22	1197826	-2094	1194276	-44	1194276	-44		
42	$2p3d \ 3P_1^o$	1200470	1200102	-368	1200258	-212	1200366	-104	1198239	-2231	1200580	110	1200580	110		
43	$2p3d \ 3P_0^o$	1200750	1200339	-411	1200498	-252	1200602	-148	1198448	-2302	1200580	110	1200580	110		
44	$2p3p \ 1S_0$	1206150	1205819	-331	1205105	-1045	1206371	221	1208729	2579	1204783	-1367	1204783	-1367		
45	$2p3d \ 1F_3^o$	1212060	1212072	12	1211725	-335	1212284	224	1213188	1128	1210313	-1747	1210313	-1747		
46	$2p3d \ 1P_1^o$	1218430	1218082	-348	1217714	-716	1218654	224	1218913	483	1218192	-238	1218192	-238		
47	$2s4s \ 3S_1$	1299170	1298906	-264	1299150	-20	1298876	-294	1294890	-4280	1294890	-4280	1294890	-4280		
48	$2s4s \ 1S_0$	1307080	1306994	-86	1307171	91	1307024	-56	1303810	-3270	1303810	-3270	1303810	-3270		
49	$2s4p \ 3P_0^o$	...	1317970	...	1318161	...	1317955	...	1314158	...	1314158	...	1314158	...		
50	$2s4p \ 3P_1^o$	...	1318016	...	1318199	...	1318001	...	1314207	...	1314207	...	1314207	...		
51	$2s4p \ 3P_2^o$	1318110	1318126	16	1318319	209	1318111	1	1314311	-3799	1314311	-3799	1314311	-3799		
52	$2s4p \ 1P_1^o$	1319890	1319731	-159	1319754	-136	1319731	-159	1316644	-3246	1316644	-3246	1316644	-3246		

Table 3 continued

**Table 3** (*continued*)

Key	Level	NIST		MCDHF/RCI		MBPT		MBPT2		AUTOSTRUCTURE		MBPT3		MCHF/BP	
		E	E	E	ΔE	E	ΔE	E	ΔE	E	ΔE	E	ΔE	E	ΔE
53	$2s4d\ ^3D_1$	1328390	1328043	-347	1328252	-138	1328014	-376	1324414	-3976	...	...	...	...	...
54	$2s4d\ ^3D_2$	1328265	1328057	-208	1328255	-10	1328028	-237	1324433	-3832	...	...	...	...	...
55	$2s4d\ ^3D_3$	1328318	1328082	-236	1328284	-34	1328053	-265	1324461	-3857	...	...	...	...	...
56	$2s4d\ ^1D_2$	1333900	1333874	-26	1333798	-102	1333888	-12	1331200	-2700	...	...	...	...	...
57	$2s4f\ ^3F_2^o$	1335190	1335111	-79	1335327	137	1335090	-100	1331242	-3948	...	...	...	...	...
58	$2s4f\ ^3F_3^o$	1335300	1335119	-181	1335334	34	1335097	-203	1331255	-4045	...	...	...	...	...
59	$2s4f\ ^3F_4^o$	1335347	1335132	-215	1335347	0	1335110	-237	1331272	-4075	...	...	...	...	...
60	$2s4f\ ^1F_3^o$	1337056	1336905	-151	1336999	-57	1336904	-152	1333527	-3529	...	...	...	...	...
61	$2p4s\ ^3P_0^o$	1430600	1430746	146	1430940	340	1430892	292	1427997	-2603	...	...	...	...	...
62	$2p4s\ ^3P_1^o$	1431010	1431042	32	1431215	205	1431185	175	1428345	-2665	...	...	...	...	...
63	$2p4s\ ^3P_2^o$	1431990	1432355	365	1432557	567	1432496	506	1429637	-2353	...	...	...	...	...
64	$2p4s\ ^1P_1^o$	1433330	1433369	39	1433465	135	1433490	160	1430986	-2344	...	...	...	...	...
65	$2s5s\ ^3S_1$	1436460	1436099	-361	1436357	-103	1436250	-210	1432279	-4181	...	...	...	...	...
66	$2s5s\ ^1S_0$	1439400	1438826	-574	1439030	-370	1439010	-390	1434823	-4577	...	...	...	...	...
67	$2p4p\ ^1P_1$	1443980	1443735	-245	1443964	-16	1443897	-83	1441081	-2899	...	...	...	...	...
68	$2p4p\ ^3D_1$	1445400	1445277	-123	1445494	94	1445433	33	1442679	-2721	...	...	...	...	...
69	$2p4p\ ^3D_2$	1445700	1445610	-90	1445818	118	1445765	65	1443021	-2679	...	...	...	...	...
70	$2p4p\ ^3D_3$	1446760	1446554	-206	1446772	12	1446705	-55	1443942	-2818	...	...	...	...	...
71	$2s5p\ ^3P_0^o$	...	1446973	1447186	...	1447217	...	1442987	...	...	...	...	...	...	...
72	$2s5p\ ^3P_1^o$	...	1446984	1447193	...	1447228	...	1442999	...	...	...	...	...	...	...
73	$2s5p\ ^3P_2^o$	...	1447007	1447222	...	1447253	...	1443021	...	...	...	...	...	...	...
74	$2s5p\ ^1P_1^o$	1450500	1450833	333	1450694	194	1451111	611	1448154	-2346	...	...	...	...	...
75	$2p4p\ ^3P_0$	1450600	1450874	274	1450895	295	1451051	451	1448434	-2166	...	...	...	...	...
76	$2p4p\ ^3P_1$	1451130	1450992	-138	1451044	-86	1451173	43	1448459	-2671	...	...	...	...	...
77	$2p4p\ ^3P_2$	1452180	1451781	-399	1451818	-362	1451954	-226	1449104	-3076	...	...	...	...	...
78	$2p4p\ ^3S_1$	1452590	1452229	-361	1452351	-239	1452420	-170	1449117	-3473	...	...	...	...	...
79	$2s5d\ ^3D_1$	1452900	1452978	78	1453211	311	1453191	291	1449590	-3310	...	...	...	...	...
80	$2s5d\ ^3D_2$	1453100	1452995	-105	1453217	117	1453207	107	1449421	-3679	...	...	...	...	...
81	$2p4d\ ^3F_2^o$	1452990	1453024	34	1453219	229	1453128	138	1449902	-3088	...	...	...	...	...
82	$2s5d\ ^3D_3$	1453200	1453025	-175	1453247	47	1453231	31	1449199	-4001	...	...	...	...	...
83	$2s5g\ ^3G_3$	1453680	1453199	-481	1453433	-247	1453237	-443	1449294	-4386	...	...	...	...	...
84	$2s5g\ ^3G_4$	1453300	1453257	-43	1453486	186	1453287	-13	1449355	-3945	...	...	...	...	...
85	$2p4d\ ^3F_3^o$	1453710	1453375	-335	1453567	-143	1453475	-235	1450137	-3573	...	...	...	...	...
86	$2s5g\ ^3G_5$	1453710	1453496	-214	1453732	22	1453521	-189	1449546	-4164	...	...	...	...	...
87	$2s5g\ ^1G_4$	...	1453566	1453790	...	1453591	...	1449635	...	...	...	...	...	...	...
88	$2s5f\ ^3F_4^o$	1454010	1453809	-201	1454016	6	1453906	-104	1450425	-3585	...	...	...	...	...
89	$2s5f\ ^1F_3^o$	1454950	1454855	-95	1455027	77	1454947	-3	1451050	-3900	...	...	...	...	...
90	$2s5d\ ^1D_2$	1455400	1454971	-429	1454996	-404	1455192	-208	1451844	-3556	...	...	...	...	...
91	$2p4d\ ^1D_2^o$	1455930	1455742	-188	1455970	40	1455891	-39	1452958	-2972	...	...	...	...	...
92	$2p4p\ ^1D_2$	1456680	1456542	-138	1456317	-363	1456733	53	1454691	-1989	...	...	...	...	...
93	$2s5f\ ^3F_2^o$	1458260	1457897	-363	1458092	-168	1458013	-247	1454844	-3416	...	...	...	...	...
94	$2s5f\ ^3F_3^o$	1458419	1458067	-352	1458252	-167	1458183	-236	1455088	-3331	...	...	...	...	...
95	$2p4d\ ^3F_4^o$	1458703	1458479	-224	1458665	-38	1458593	-110	1455675	-3028	...	...	...	...	...
96	$2p4d\ ^3D_1^o$	1460600	1460317	-283	1460527	-73	1460498	-102	1457501	-3099	...	...	...	...	...
97	$2p4d\ ^3D_2^o$	1461110	1460552	-558	1460764	-346	1460730	-380	1457746	-3364	...	...	...	...	...
98	$2p4d\ ^3D_3^o$	1461220	1460970	-250	1461179	-41	1461145	-75	1458171	-3049	...	...	...	...	...
99	$2p4f\ ^1F_3$	1462080	1461766	-314	1462008	-72	1461929	-151	1458781	-3299	...	...	...	...	...
100	$2p4f\ ^3F_2$	1462080	1461890	-190	1462121	41	1462058	-22	1458975	-3105	...	...	...	...	...
101	$2p4f\ ^3F_3$	1462830	1462168	-662	1462408	-422	1462330	-500	1459227	-3603	...	...	...	...	...
102	$2p4f\ ^3F_4$	1462550	1462286	-264	1462521	-29	1462449	-101	1459372	-3178	...	...	...	...	...
103	$2p4d\ ^3P_2^o$	1462930	1463091	161	1463261	331	1463286	356	1460502	-2428	...	...	...	...	...
104	$2p4d\ ^3P_1^o$	1463390	1463451	61	1463615	225	1463645	255	1460868	-2522	...	...	...	...	...
105	$2p4d\ ^3P_0^o$	1464180	1463646	-534	1463809	-371	1463840	-340	1461058	-3122	...	...	...	...	...
106	$2p4f\ ^3D_3$	1466640	1466327	-313	1466543	-97	1466494	-146	1463545	-3095	...	...	...	...	...
107	$2p4f\ ^3G_3$	1466670	1466383	-287	1466576	-94	1466498	-172	1463854	-2816	...	...	...	...	...
108	$2p4p\ ^1S_0$	...	1466386	1465339	...	1466721	...	1466911	...	...	...	...	...	...	...
109	$2p4f\ ^3G_4$	1466569	1466595	26	1466763	194	1466709	140	1464139	-2430	...	...	...	...	...
110	$2p4f\ ^3D_2$	1467230	1466598	-632	1466788	-442	1466772	-458	1463876	-3354	...	...	...	...	...
111	$2p4f\ ^3D_1$	...	1467077	1467296	...	1467243	...	1464297	...	...	...	...	...	...	...
112	$2p4f\ ^3G_5$	1467457	1467252	-205	1467446	-11	1467364	-93	1464800	-2657	...	...	...	...	...

Table 3 continued

**Table 3** (*continued*)

Key	Level	NIST		MCDHF/RCI		MBPT		MBPT2		AUTOSTRUCTURE		MBPT3		MCHF/BP	
		E	E	E	$\Delta E$	E	$\Delta E$	E	$\Delta E$	E	$\Delta E$	E	$\Delta E$	E	$\Delta E$
113	$2p4f\ ^1D_2$	1467730	1467610	-120	1467720	-10	1467802	72	1465250	-2480	...	...	...	...	...
114	$2p4f\ ^1G_4$	1467946	1467806	-140	1467865	-81	1467932	-14	1465842	-2104	...	...	...	...	...
115	$2p4d\ ^1F_3^o$	1469550	1469623	73	1469287	-263	1469686	136	1469043	-507	...	...	...	...	...
116	$2p4d\ ^1P_1^o$	1470080	1470147	67	1469991	-89	1470417	337	1468642	-1438	...	...	...	...	...
117	$2s6s\ ^3S_1$	1512110	1512005	-105	1512243	133	1511966	-144	1507823	-4287	...	...	...	...	...
118	$2s6s\ ^1S_0$	...	1514042		1514038	...	1514984	...	1510200	...	...	...	...	...	...
119	$2s6p\ ^3P_0^o$	...	1517319		1517515	...	1517282	...	1513139	...	...	...	...	...	...
120	$2s6p\ ^3P_1^o$	1517740	1517332	-408	1517527	-213	1517303	-437	1513152	-4588	...	...	...	...	...
121	$2s6p\ ^3P_2^o$	1517741	1517363	-378	1517562	-179	1517357	-384	1513180	-4561	...	...	...	...	...
122	$2s6p\ ^1P_1^o$	1518600	1517824	-776	1517866	-734	1517802	-798	1513890	-4710	...	...	...	...	...
123	$2s6d\ ^3D_1$	1520100	1520185	85	1520430	330	1520187	87	1516069	-4031	...	...	...	...	...
124	$2s6d\ ^3D_2$	1520360	1520189	-171	1520425	65	1520191	-169	1516074	-4286	...	...	...	...	...
125	$2s6d\ ^3D_3$	1520460	1520196	-264	1520430	-30	1520199	-261	1516082	-4378	...	...	...	...	...
126	$2s6d\ ^1D_2$	1521860	1521680	-180	1521714	-146	1521667	-193	1517798	-4062	...	...	...	...	...
127	$2s6f\ ^3F_2^o$	1522402	1521981	-421	1522219	-183	1521975	-427	...	...	...	...	...	...	...
128	$2s6f\ ^3F_3^o$	...	1521984		1522221	...	1521977	...	...	...	...	...	...	...	...
129	$2s6f\ ^3F_4^o$	...	1521987		1522225	...	1521981	...	...	...	...	...	...	...	...
130	$2s6h\ ^3H_4^o$	...	1522131		1522378	...	1522144	...	...	...	...	...	...	...	...
131	$2s6h\ ^3H_5^o$	1522421	1522133	-288	1522379	-42	1522145	-276	...	...	...	...	...	...	...
132	$2s6h\ ^1H_5^o$	1522420	1522134	-286	1522380	-40	1522146	-274	...	...	...	...	...	...	...
133	$2s6h\ ^3H_6^o$	...	1522135		1522381	...	...	...	...	...	...	...	...	...	...
134	$2s6g\ ^3G_3$	...	1522380		1522618	...	1522359	...	...	...	...	...	...	...	...
135	$2s6g\ ^3G_4$	...	1522384		1522622	...	1522363	...	...	...	...	...	...	...	...
136	$2s6g\ ^3G_5$	...	1522390		1522627	...	1522369	...	...	...	...	...	...	...	...
137	$2s6g\ ^1G_4$	...	1522406		1522635	...	1522385	...	...	...	...	...	...	...	...
138	$2s6f\ ^1F_3^o$	1523040	1522569	-471	1522746	-294	1522564	-476	...	...	...	...	...	...	...

**Table 4.** Computed excitation energies for the  $n \leq 3$  levels of the ions from B II to Ne VII from the present MCDHF/RCI calculations, and from the calculations by Safranova et al. (1996, 1997) [MBPT3], and by Tachiev & Froese Fischer (1999); Froese Fischer & Tachiev (2004) [MCHF/BP] are compared with the NIST compiled values.  $E$  – excitation energies from different resources ;  $\Delta E$  – the differences between the calculated energies from different resources and the NIST compiled values.

Z	Key	Level	NIST		MCDHF/RCI		MBPT3		MCHF/BP	
			E	$\Delta E$	E	$\Delta E$	E	$\Delta E$	E	$\Delta E$
5	1	$2s^2\ ^1S_0$	0	...	0	...	0	...	0	...
5	2	$2s2p\ ^3P_0^o$	37335.54	-9.54	37326	-9.54	36624	-711.54	37468	132.46
5	3	$2s2p\ ^3P_1^o$	37341.65	-10.65	37331	-10.65	36631	-710.65	37475	133.35
5	4	$2s2p\ ^3P_2^o$	37357.8	-10.8	37347	-10.8	36648	-709.8	37491	133.2
5	5	$2s2p\ ^1P_1^o$	73396.51	73670	273.49	70046	-3350.51	73583	186.49	
5	6	$2p^2\ ^3P_0$	98911.38	98911	-0.38	98042	-869.38	99236	324.62	
5	7	$2p^2\ ^3P_1$	98919.87	98919	-0.87	98051	-868.87	99245	325.13	
5	8	$2p^2\ ^3P_2$	98933.26	98932	-1.26	98066	-867.26	99258	324.74	
5	9	$2p^2\ ^1D_2$	102362.77	102588	225.23	98608	-3754.77	102702	339.23	
5	10	$2p^2\ ^1S_0$	127661.19	127854	192.81	125993	-1668.19	127993	331.81	
5	11	$2s3s\ ^3S_1$	129773.83	129753	-20.83	...	...	129913	139.17	
5	12	$2s3s\ ^1S_0$	137622.25	137790	167.75	...	...	137859	236.75	
5	13	$2s3p\ ^3P_0^o$	143989.95	143948	-41.95	...	...	144149	159.05	
5	14	$2s3p\ ^3P_1^o$	143990.56	143949	-41.56	...	...	144150	159.44	
5	15	$2s3p\ ^3P_2^o$	143994.11	143953	-41.11	...	...	144154	159.89	
5	16	$2s3p\ ^1P_1^o$	144102.94	144102	-0.94	...	...	144278	175.06	

*Table 4 continued*

**Table 4** (*continued*)

Z	Key	Level	NIST		MCDHF/RCI		MBPT3		MCHF/BP	
			E	E	E	ΔE	E	ΔE	E	ΔE
5	17	$2s3d\ ^3D_1$	150649.68	150637	-12.68	...	...	...	150837	187.32
5	18	$2s3d\ ^3D_2$	150649.68	150637	-12.68	...	...	...	150837	187.32
5	19	$2s3d\ ^3D_3$	150649.68	150638	-11.68	...	...	...	150837	187.32
5	20	$2s3d\ ^1D_2$	154686.12	154725	38.88	...	...	...	154881	194.88
5	37	$2p3s\ ^3P_0^\circ$	181645.9	181636	-9.9	...	...	...	...	...
5	38	$2p3s\ ^3P_1^\circ$	181655.55	181646	-9.55	...	...	...	...	...
5	39	$2p3s\ ^3P_2^\circ$	181676.76	181668	-8.76	...	...	...	...	...
5	56	$2p3s\ ^1P_1^\circ$	186629.92	187139	509.08	...	...	...	...	...
5	59	$2p3p\ ^1P_1$	189127.98	189098	-29.98	...	...	...	...	...
5	80	$2p3p\ ^3D_1$	191034.8	191048	13.2	...	...	...	...	...
5	81	$2p3p\ ^3D_2$	191044.6	191059	14.4	...	...	...	...	...
5	82	$2p3p\ ^3D_3$	191063.4	191077	13.6	...	...	...	...	...
5	83	$2p3p\ ^3S_1$	193226.5	194257	1030.5	...	...	...	...	...
5	84	$2p3p\ ^3P_0$	195601.7	195666	64.3	...	...	...	...	...
5	85	$2p3p\ ^3P_1$	195608.22	195672	63.78	...	...	...	...	...
5	86	$2p3p\ ^3P_2$	195619.05	195683	63.95	...	...	...	...	...
5	87	$2p3p\ ^1D_2$	196979.6	197493	513.4	...	...	...	...	...
5	88	$2p3d\ ^1D_2^\circ$	197720.14	197717	-3.14	...	...	...	...	...
5	89	$2p3d\ ^3F_2^\circ$	197694.7	197876	181.3	...	...	...	...	...
5	90	$2p3d\ ^3F_3^\circ$	197703.7	197885	181.3	...	...	...	...	...
5	91	$2p3d\ ^3F_4^\circ$	197718.7	197898	179.3	...	...	...	...	...
5	92	$2p3d\ ^3D_1^\circ$	200478.1	200464	-14.1	...	...	...	...	...
5	93	$2p3d\ ^3D_2^\circ$	200481.9	200468	-13.9	...	...	...	...	...
5	94	$2p3d\ ^3D_3^\circ$	200487.28	200474	-13.28	...	...	...	...	...
5	95	$2p3d\ ^3P_2^\circ$	...	202702	...	...	...	...	...	...
5	96	$2p3d\ ^3P_1^\circ$	...	202711	...	...	...	...	...	...
5	97	$2p3d\ ^3P_0^\circ$	200726.6	202716	1989.4	...	...	...	...	...
5	98	$2p3d\ ^1F_3^\circ$	...	203171	...	...	...	...	...	...
5	99	$2p3p\ ^1S_0$	203130	204292	1162	...	...	...	...	...
5	100	$2p3d\ ^1P_1^\circ$	205107	205308	201	...	...	...	...	...
6	1	$2s^2\ ^1S_0$	0	0	...	0	...	0	...	...
6	2	$2s2p\ ^3P_0^\circ$	52367.06	52355	-12.06	51916	-451.06	52391	23.94	
6	3	$2s2p\ ^3P_1^\circ$	52390.75	52378	-12.75	51940	-450.75	52415	24.25	
6	4	$2s2p\ ^3P_2^\circ$	52447.11	52434	-13.11	51997	-450.11	52472	24.89	
6	5	$2s2p\ ^1P_1^\circ$	102352.04	102559	206.96	99710	-2642.04	102446	93.96	
6	6	$2p^2\ ^3P_0$	137425.7	137424	-1.7	136843	-582.7	137667	241.3	
6	7	$2p^2\ ^3P_1$	137454.4	137453	-1.4	136872	-582.4	137696	241.6	
6	8	$2p^2\ ^3P_2$	137502.01	137500	-2.01	136923	-579.01	137744	241.99	
6	9	$2p^2\ ^1D_2$	145876.13	146005	128.87	143146	-2730.13	146152	275.87	
6	10	$2p^2\ ^1S_0$	182519.88	182796	276.12	180140	-2379.88	182879	359.12	
6	11	$2s3s\ ^3S_1$	238213	238186	-27	238878	665	238282	69	
6	12	$2s3s\ ^1S_0$	247170.26	247173	2.74	250099	2928.74	247271	100.74	
6	13	$2s3p\ ^1P_1^\circ$	258931.29	258917	-14.29	259312	380.71	259034	102.71	
6	14	$2s3p\ ^3P_0^\circ$	259705.55	259670	-35.55	...	...	259793	87.45	
6	15	$2s3p\ ^3P_1^\circ$	259711.22	259676	-35.22	260043	331.78	259799	87.78	
6	16	$2s3p\ ^3P_2^\circ$	259724.3	259689	-35.3	...	...	259812	87.7	
6	17	$2s3d\ ^3D_1$	270010.83	269997	-13.83	...	...	270136	125.17	
6	18	$2s3d\ ^3D_2$	270011.93	269998	-13.93	269932	-79.93	270137	125.07	

Table 4 continued

**Table 4** (*continued*)

Z	Key	Level	NIST		MCDHF/RCI		MBPT3		MCHF/BP	
			E	E	ΔE	E	ΔE	E	ΔE	
6	19	$2s3d\ ^3D_3$	270014.74	270001	-13.74	...	...	270140	125.26	
6	20	$2s3d\ ^1D_2$	276482.86	276521	38.14	275941	-541.86	276621	138.14	
6	21	$2p3s\ ^3P_0^{\circ}$	308216.58	308182	-34.58	...	...	...	...	
6	22	$2p3s\ ^3P_1^{\circ}$	308248.91	308214	-34.91	308212	-36.91	...	...	
6	23	$2p3s\ ^3P_2^{\circ}$	308317.29	308282	-35.29	...	...	...	...	
6	25	$2p3s\ ^1P_1^{\circ}$	310006.32	309998	-8.32	310972	965.68	...	...	
6	30	$2p3p\ ^1P_1$	319720.35	319690	-30.35	319746	25.65	...	...	
6	39	$2p3p\ ^3D_1$	323076.88	323063	-13.88	...	...	...	...	
6	40	$2p3p\ ^3D_2$	323101.36	323088	-13.36	322384	-717.36	...	...	
6	41	$2p3p\ ^3D_3$	323140.33	323127	-13.33	...	...	...	...	
6	43	$2p3p\ ^3S_1$	327278.27	327276	-2.27	324668	-2610.27	...	...	
6	44	$2p3p\ ^3P_0$	329685.38	329655	-30.38	...	...	...	...	
6	45	$2p3p\ ^3P_1$	329706.47	329676	-30.47	329762	55.53	...	...	
6	46	$2p3p\ ^3P_2$	329743.57	329714	-29.57	...	...	...	...	
6	47	$2p3d\ ^1D_2^{\circ}$	332691.28	332653	-38.28	332995	303.72	...	...	
6	48	$2p3p\ ^1D_2$	333118.21	333215	96.79	331472	-1646.21	...	...	
6	49	$2p3d\ ^3F_2^{\circ}$	333387.01	333458	70.99	...	...	...	...	
6	50	$2p3d\ ^3F_3^{\circ}$	333411.55	333483	71.45	329619	-3792.55	...	...	
6	51	$2p3d\ ^3F_4^{\circ}$	333447.24	333519	71.76	...	...	...	...	
6	52	$2p3d\ ^3D_1^{\circ}$	337655.98	337608	-47.98	...	...	...	...	
6	53	$2p3d\ ^3D_2^{\circ}$	337668.89	337621	-47.89	337754	85.11	...	...	
6	54	$2p3d\ ^3D_3^{\circ}$	337688.04	337640	-48.04	...	...	...	...	
6	57	$2p3d\ ^3P_2^{\circ}$	340101.84	340083	-18.84	...	...	...	...	
6	58	$2p3d\ ^3P_1^{\circ}$	340127.53	340109	-18.53	339948	-179.53	...	...	
6	59	$2p3d\ ^3P_0^{\circ}$	340141.83	340123	-18.83	...	...	...	...	
6	60	$2p3d\ ^1F_3^{\circ}$	341370.94	341502	131.06	333225	-8145.94	...	...	
6	65	$2p3p\ ^1S_0$	345095.43	345412	316.57	329393	-15702.43	...	...	
6	74	$2p3d\ ^1P_1^{\circ}$	346712.73	346816	103.27	344161	-2551.73	...	...	
7	1	$2s^2\ ^1S_0$	0	0	...	0	...	0	...	
7	2	$2s2p\ ^3P_0^{\circ}$	67209.2	67186	-23.2	66898	-311.2	67235	25.8	
7	3	$2s2p\ ^3P_1^{\circ}$	67272.3	67248	-24.3	66962	-310.3	67298	25.7	
7	4	$2s2p\ ^3P_2^{\circ}$	67416.3	67392	-24.3	67107	-309.3	67442	25.7	
7	5	$2s2p\ ^1P_1^{\circ}$	130693.9	130870	176.1	128534	-2159.9	130800	106.1	
7	6	$2p^2\ ^3P_0$	175535.4	175506	-29.4	175117	-418.4	175806	270.6	
7	7	$2p^2\ ^3P_1$	175608.1	175579	-29.1	175191	-417.1	175880	271.9	
7	8	$2p^2\ ^3P_2$	175732.9	175703	-29.9	175318	-414.9	176004	271.1	
7	9	$2p^2\ ^1D_2$	188882.5	188954	71.5	186764	-2118.5	189203	320.5	
7	10	$2p^2\ ^1S_0$	235369.3	235571	201.7	233393	-1976.3	235798	428.7	
7	11	$2s3s\ ^3S_1$	377284.8	377241	-43.8	377662	377.2	377393	108.2	
7	12	$2s3s\ ^1S_0$	388854.6	388823	-31.6	390012	1157.4	389007	152.4	
7	13	$2s3p\ ^1P_1^{\circ}$	404522.4	404497	-25.4	404641	118.6	404665	142.6	
7	14	$2s3p\ ^3P_0^{\circ}$	405971.6	405930	-41.6	...	...	406096	124.4	
7	15	$2s3p\ ^3P_1^{\circ}$	405987.5	405946	-41.5	406217	229.5	406112	124.5	
7	16	$2s3p\ ^3P_2^{\circ}$	406022.8	405982	-40.8	...	...	406148	125.2	
7	17	$2s3d\ ^3D_1$	420045.8	420020	-25.8	...	...	420210	164.2	
7	18	$2s3d\ ^3D_2$	420049.6	420024	-25.6	420035	-14.6	420214	164.4	
7	19	$2s3d\ ^3D_3$	420058	420032	-26	...	...	420222	164	
7	20	$2s3d\ ^1D_2$	429159.6	429192	32.4	428628	-531.6	429340	180.4	

Table 4 continued

**Table 4** (*continued*)

Z	Key	Level	NIST		MCDHF/RCI		MBPT3		MCHF/BP	
			E	E	ΔE	E	ΔE	E	ΔE	E
7	21	$2p3s\ ^3P_0^o$	465291.8	465247	-44.8	...	...	...	...	...
7	22	$2p3s\ ^3P_1^o$	465371	465325	-46	465418	47	...	...	...
7	23	$2p3s\ ^3P_2^o$	465536.6	465491	-45.6	...	...	...	...	...
7	24	$2p3s\ ^1P_1^o$	473029.3	473064	34.7	472347	-682.3	...	...	...
7	25	$2p3p\ ^1P_1$	480884.2	480830	-54.2	480988	103.8	...	...	...
7	26	$2p3p\ ^3D_1$	484498.2	484464	-34.2	...	...	...	...	...
7	27	$2p3p\ ^3D_2$	484594.9	484561	-33.9	484592	-2.9	...	...	...
7	28	$2p3p\ ^3D_3$	484746.2	484713	-33.2	...	...	...	...	...
7	29	$2p3p\ ^3S_1$	498045.5	487594	-10451.5	489510	-8535.5	...	...	...
7	30	$2p3p\ ^3P_0$	494253.1	494201	-52.1	...	...	...	...	...
7	31	$2p3p\ ^3P_1$	494309.2	494257	-52.2	494427	117.8	...	...	...
7	32	$2p3p\ ^3P_2$	494402	494350	-52	...	...	...	...	...
7	34	$2p3d\ ^3F_2^o$	495406.2	495409	2.8	...	...	...	...	...
7	35	$2p3d\ ^3F_3^o$	495482.6	495485	2.4	496437	954.4	...	...	...
7	36	$2p3d\ ^3F_4^o$	495585.7	495588	2.3	...	...	...	...	...
7	38	$2p3d\ ^1D_2^o$	498310.3	498261	-49.3	498622	311.7	...	...	...
7	39	$2p3p\ ^1D_2$	499705.9	499729	23.1	498612	-1093.9	...	...	...
7	43	$2p3d\ ^3D_1^o$	505554	505497	-57	...	...	...	...	...
7	44	$2p3d\ ^3D_2^o$	505588.2	505531	-57.2	505729	140.8	...	...	...
7	45	$2p3d\ ^3D_3^o$	505630.6	505573	-57.6	...	...	...	...	...
7	46	$2p3d\ ^1F_3^o$	506284.8	506301	16.2	507701	1416.2	...	...	...
7	51	$2p3d\ ^3P_2^o$	511509.3	511489	-20.3	...	...	...	...	...
7	52	$2p3d\ ^3P_1^o$	511560.4	511539	-21.4	509228	-2332.4	...	...	...
7	53	$2p3d\ ^3P_0^o$	511591.2	511569	-22.2	...	...	...	...	...
7	55	$2p3p\ ^1S_0$	515569.8	515734	164.2	505783	-9786.8	...	...	...
7	59	$2p3d\ ^1P_1^o$	518610.5	518689	78.5	516780	-1830.5	...	...	...
8	1	$2s^2\ ^1S_0$	0	0	...	0	...	0	...	...
8	2	$2s2p\ ^3P_0^o$	81942.5	81887	-55.5	81718	-224.5	81985	42.5	
8	3	$2s2p\ ^3P_1^o$	82078.6	82023	-55.6	81856	-222.6	82122	43.4	
8	4	$2s2p\ ^3P_2^o$	82385.3	82329	-56.3	82164	-221.3	82429	43.7	
8	5	$2s2p\ ^1P_1^o$	158797.7	158936	138.3	156979	-1818.7	158933	135.3	
8	6	$2p^2\ ^3P_0$	213462.5	213400	-62.5	213149	-313.5	213794	331.5	
8	7	$2p^2\ ^3P_1$	213618.2	213556	-62.2	213306	-312.2	213951	332.8	
8	8	$2p^2\ ^3P_2$	213887	213824	-63	213578	-309	214220	333	
8	9	$2p^2\ ^1D_2$	231721.4	231759	37.6	230003	-1718.4	232120	398.6	
8	10	$2p^2\ ^1S_0$	287910.3	288132	221.7	286249	-1661.3	288434	523.7	
8	11	$2s3s\ ^3S_1$	546972.7	546897	-75.7	547283	310.3	547153	180.3	
8	12	$2s3s\ ^1S_0$	561276.4	561219	-57.4	562020	743.6	561500	223.6	
8	13	$2s3p\ ^1P_1^o$	580824.9	580763	-61.9	580863	38.1	581027	202.1	
8	14	$2s3p\ ^3P_0^o$	582806.4	582731	-75.4	...	...	582986	179.6	
8	15	$2s3p\ ^3P_1^o$	582843.1	582768	-75.1	583048	204.9	583023	179.9	
8	16	$2s3p\ ^3P_2^o$	582920.3	582845	-75.3	...	...	583100	179.7	
8	17	$2s3d\ ^3D_1$	600748.9	600687	-61.9	...	...	600964	215.1	
8	18	$2s3d\ ^3D_2$	600758.9	600697	-61.9	600776	17.1	600974	215.1	
8	19	$2s3d\ ^3D_3$	600779.2	600717	-62.2	...	...	600994	214.8	
8	20	$2s3d\ ^1D_2$	612615.6	612621	5.4	612120	-495.6	612856	240.4	
8	21	$2p3s\ ^3P_0^o$	652918	652830	-88	...	...	...	...	
8	22	$2p3s\ ^3P_1^o$	653080.1	652992	-88.1	653173	92.9	...	...	

Table 4 continued

**Table 4** (*continued*)

Z	Key	Level	NIST		MCDHF/RCI		MBPT3		MCHF/BP	
			E	E	ΔE	E	ΔE	E	ΔE	
8	23	$2p3s\ ^3P_2^o$	653423.3	653335	-88.3	...	...	...	...	...
8	24	$2p3s\ ^1P_1^o$	664485.9	664481	-4.9	663710	-775.9	...	...	...
8	25	$2p3p\ ^1P_1$	672693.8	672605	-88.8	672841	147.2	...	...	...
8	26	$2p3p\ ^3D_1$	677150.7	677075	-75.7	...	...	...	...	...
8	27	$2p3p\ ^3D_2$	677348.5	677272	-76.5	677385	36.5	...	...	...
8	28	$2p3p\ ^3D_3$	677665	677589	-76	...	...	...	...	...
8	29	$2p3p\ ^3S_1$	683942.9	683872	-70.9	684188	245.1	...	...	...
8	30	$2p3p\ ^3P_0$	689403.5	689312	-91.5	...	...	...	...	...
8	31	$2p3p\ ^3P_1$	689517.7	689426	-91.7	689662	144.3	...	...	...
8	32	$2p3p\ ^3P_2$	689708.5	689617	-91.5	...	...	...	...	...
8	33	$2p3d\ ^3F_2^o$	692626	692568	-58	...	...	...	...	...
8	34	$2p3d\ ^3F_3^o$	692809.4	692751	-58.4	693159	349.6	...	...	...
8	35	$2p3d\ ^3F_4^o$	693044.8	692986	-58.8	...	...	...	...	...
8	36	$2p3d\ ^1D_2^o$	694643.8	694558	-85.8	694956	312.2	...	...	...
8	37	$2p3p\ ^1D_2$	697170.2	697138	-32.2	696264	-906.2	...	...	...
8	38	$2p3d\ ^3D_1^o$	704182	704079	-103	...	...	...	...	...
8	39	$2p3d\ ^3D_2^o$	704242	704147	-95	704414	172	...	...	...
8	40	$2p3d\ ^3D_3^o$	704348	704252	-96	...	...	...	...	...
8	41	$2p3p\ ^1S_0$	707635.5	707609	-26.5	708679	1043.5	...	...	...
8	42	$2p3d\ ^3P_2^o$	707981.2	707904	-77.2	...	...	...	...	...
8	43	$2p3d\ ^3P_1^o$	708125.1	708048	-77.1	708875	749.9	...	...	...
8	44	$2p3d\ ^3P_0^o$	708205	708128	-77	...	...	...	...	...
8	45	$2p3d\ ^1F_3^o$	712963.5	712969	5.5	711357	-1606.5	...	...	...
8	46	$2p3d\ ^1P_1^o$	719274.9	719298	23.1	719805	530.1	...	...	...
9	1	$2s^2\ ^1S_0$	0	0	...	0	...	0	...	...
9	2	$2s2p\ ^3P_0^o$	96590	96560	-30	96447	-143	96704	114	
9	3	$2s2p\ ^3P_1^o$	96850	96820	-30	96709	-141	96966	116	
9	4	$2s2p\ ^3P_2^o$	97427	97396	-31	97287	-140	97544	117	
9	5	$2s2p\ ^1P_1^o$	186844	186965	121	185279	-1565	187040	196	
9	6	$2p^2\ ^3P_0$	251336	251293	-43	251116	-220	251819	483	
9	7	$2p^2\ ^3P_1$	251629	251588	-41	251412	-217	252116	487	
9	8	$2p^2\ ^3P_2$	252139	252097	-42	251926	-213	252626	487	
9	9	$2p^2\ ^1D_2$	274602	274635	33	273165	-1437	275151	549	
9	10	$2p^2\ ^1S_0$	340434	340642	208	339008	-1426	341113	679	
9	11	$2s3s\ ^3S_1$	747284	747216	-68	747571	287	747606	322	
9	12	$2s3s\ ^1S_0$	764392	764321	-71	764937	545	764736	344	
9	13	$2s3p\ ^1P_1^o$	787844	787780	-64	787849	5	788139	295	
9	14	$2s3p\ ^3P_0^o$	790240	790172	-68	...	...	790516	276	
9	15	$2s3p\ ^3P_1^o$	790312	790244	-68	790515	203	790589	277	
9	16	$2s3p\ ^3P_2^o$	790460	790391	-69	...	...	790737	277	
9	17	$2s3d\ ^3D_1$	812142	812084	-58	...	...	812446	304	
9	18	$2s3d\ ^3D_2$	812166	812105	-61	812204	38	812467	301	
9	19	$2s3d\ ^3D_3$	812202	812146	-56	...	...	812507	305	
9	20	$2s3d\ ^1D_2$	826843	826845	2	826384	-459	827168	325	
9	21	$2p3s\ ^3P_0^o$	871140	871065	-75	...	...	...	...	...
9	22	$2p3s\ ^3P_1^o$	871437	871361	-76	871571	134	...	...	...
9	23	$2p3s\ ^3P_2^o$	872084	871996	-88	...	...	...	...	...
9	24	$2p3s\ ^1P_1^o$	886288	886249	-39	885558	-730	...	...	...

Table 4 continued

**Table 4** (*continued*)

Z	Key	Level	NIST		MCDHF/RCI		MBPT3		MCHF/BP	
			E	E	E	ΔE	E	ΔE	E	ΔE
9	25	$2p3p\ ^1P_1$	895286	895161	-125	895417	131	...	...	...
9	26	$2p3p\ ^3D_1$	900436	900373	-63	...	...	...	...	...
9	27	$2p3p\ ^3D_2$	900791	900729	-62	900872	81	...	...	...
9	28	$2p3p\ ^3D_3$	901395	901318	-77	...	...	...	...	...
9	29	$2p3p\ ^3S_1$	909306	909264	-42	909440	134	...	...	...
9	30	$2p3p\ ^3P_0$	915181	915123	-58	...	...	...	...	...
9	31	$2p3p\ ^3P_1$	915403	915344	-59	915595	192	...	...	...
9	32	$2p3p\ ^3P_2$	915760	915693	-67	...	...	...	...	...
9	33	$2p3d\ ^3F_2^o$	...	919783	...	...	...	...	...	...
9	34	$2p3d\ ^3F_3^o$	...	920151	...	920452	...	...	...	...
9	35	$2p3d\ ^3F_4^o$	...	920598	...	...	...	...	...	...
9	36	$2p3d\ ^1D_2^o$	921824	921724	-100	922110	286	...	...	...
9	37	$2p3p\ ^1D_2$	925389	925340	-49	924624	-765	...	...	...
9	38	$2p3d\ ^3D_1^o$	933585	933493	-92	...	...	...	...	...
9	39	$2p3d\ ^3D_2^o$	933716	933620	-96	933896	180	...	...	...
9	40	$2p3d\ ^3D_3^o$	933937	933823	-114	...	...	...	...	...
9	41	$2p3d\ ^3P_2^o$	938530	938452	-78	...	...	...	...	...
9	42	$2p3d\ ^3P_1^o$	938798	938714	-84	939265	467	...	...	...
9	43	$2p3d\ ^3P_0^o$	938939	938859	-80	...	...	...	...	...
9	44	$2p3p\ ^1S_0$	934650	942260	7610	941466	6816	...	...	...
9	45	$2p3d\ ^1F_3^o$	947313	947313	0	945445	-1868	...	...	...
9	46	$2p3d\ ^1P_1^o$	953404	953422	18	953551	147	...	...	...
10	1	$2s^2\ ^1S_0$	0	0	...	0	...	0	...	...
10	2	$2s2p\ ^3P_0^o$	111252.8	111197	-55.8	111128	-124.8	111441	188.2	
10	3	$2s2p\ ^3P_1^o$	111708	111649	-59	111582	-126	111896	188	
10	4	$2s2p\ ^3P_2^o$	112702.4	112643	-59.4	112578	-124.4	112893	190.6	
10	5	$2s2p\ ^1P_1^o$	214951.6	215065	113.4	213581	-1370.6	215260	308.4	
10	6	$2p^2\ ^3P_0$	289330.4	289259	-71.4	289144	-186.4	290029	698.6	
10	7	$2p^2\ ^3P_1$	289841.1	289771	-70.1	289657	-184.1	290546	704.9	
10	8	$2p^2\ ^3P_2$	290724	290653	-71	290544	-180	291429	705	
10	9	$2p^2\ ^1D_2$	317694.6	317716	21.4	316463	-1231.6	318503	808.4	
10	10	$2p^2\ ^1S_0$	393125	393321	196	391881	-1244	394062	937	
10	11	$2s3s\ ^3S_1$	978300.29	978197	-103.29	978538	237.71	978750	449.71	
10	12	$2s3s\ ^1S_0$	998183.1	998117	-66.1	998633	449.9	998691	507.9	
10	13	$2s3p\ ^1P_1^o$	1025620.6	1025546	-74.6	1025607	-13.6	1026055	434.4	
10	14	$2s3p\ ^3P_0^o$	1028366.7	1028265	-101.7	...	...	1028751	384.3	
10	15	$2s3p\ ^3P_1^o$	1028499.59	1028397	-102.59	1028665	165.41	1028884	384.41	
10	16	$2s3p\ ^3P_2^o$	1028755.1	1028650	-105.1	...	...	1029139	383.9	
10	17	$2s3d\ ^3D_1$	1054310	1054223	-87	...	...	1054715	405	
10	18	$2s3d\ ^3D_2$	1054354.4	1054264	-90.4	1054380	25.6	1054755	400.6	
10	19	$2s3d\ ^3D_3$	1054428.3	1054337	-91.3	...	...	1054828	399.7	
10	20	$2s3d\ ^1D_2$	1071914	1071866	-48	1071447	-467	1072321	407	
10	21	$2p3s\ ^3P_0^o$	1120207	1119967	-240	...	...	...	...	...
10	22	$2p3s\ ^3P_1^o$	1120720	1120462	-258	1120697	-23	...	...	...
10	23	$2p3s\ ^3P_2^o$	1121757	1121548	-209	...	...	...	...	...
10	24	$2p3s\ ^1P_1^o$	1138860	1138711	-149	1138115	-745	...	...	...
10	25	$2p3p\ ^1P_1$	1148647	1148548	-99	1148824	177	...	...	...
10	26	$2p3p\ ^3D_1$	1154488	1154407	-81	...	...	...	...	...

Table 4 continued

**Table 4** (*continued*)

Z	Key	Level	NIST		MCDHF/RCI		MBPT3		MCHF/BP	
			E	E	ΔE	E	ΔE	E	ΔE	
10	27	$2p3p\ ^3D_2$	1155120	1154989	-131	1155162	42	...	...	...
10	28	$2p3p\ ^3D_3$	1156150	1155998	-152	...	...	...	...	...
10	29	$2p3p\ ^3S_1$	1165520	1165319	-201	1165482	-38	...	...	...
10	30	$2p3p\ ^3P_0$	1171500	1171685	185	...	...	...	...	...
10	31	$2p3p\ ^3P_1$	1172020	1172082	62	1172349	329	...	...	...
10	32	$2p3p\ ^3P_2$	1172350	1172665	315	...	...	...	...	...
10	33	$2p3d\ ^3F_2^\circ$	1177910	1177587	-323	...	...	...	...	...
10	34	$2p3d\ ^3F_3^\circ$	1178270	1178262	-8	1178542	272	...	...	...
10	35	$2p3d\ ^3F_4^\circ$	1179188	1179037	-151	...	...	...	...	...
10	36	$2p3d\ ^1D_2^\circ$	1180070	1179839	-231	1180222	152	...	...	...
10	37	$2p3p\ ^1D_2$	1185130	1184428	-702	1183838	-1292	...	...	...
10	38	$2p3d\ ^3D_1^\circ$	1194060	1193771	-289	...	...	...	...	...
10	39	$2p3d\ ^3D_2^\circ$	1194320	1193989	-331	1194276	-44	...	...	...
10	40	$2p3d\ ^3D_3^\circ$	1194538	1194354	-184	...	...	...	...	...
10	41	$2p3d\ ^3P_2^\circ$	1199920	1199678	-242	...	...	...	...	...
10	42	$2p3d\ ^3P_1^\circ$	1200470	1200102	-368	1200580	110	...	...	...
10	43	$2p3d\ ^3P_0^\circ$	1200750	1200339	-411	...	...	...	...	...
10	44	$2p3p\ ^1S_0$	1206150	1205819	-331	1204783	-1367	...	...	...
10	45	$2p3d\ ^1F_3^\circ$	1212060	1212072	12	1210313	-1747	...	...	...
10	46	$2p3d\ ^1P_1^\circ$	1218430	1218082	-348	1218192	-238	...	...	...

**Table 5.** Transition data for Be-like ions from B II to Ne VII from the present MCDHF/RCI calculations.  $\lambda$  is transition wavelength in vacuum in Å,  $S$  is line strength in atomic units,  $gf$  is weighted oscillator strength, and  $A$  is transition rate in  $s^{-1}$ . Radiative branching ratios (BR) for each transition provided by the present MCDHF/RCI calculations are listed in the last column. Only transitions contributing a fraction of more than  $10^{-5}$  to the total radiative lifetime are presented.

Z	j	i	$\lambda_{\text{MCDHF/RCI}}$	Type	$S_{\text{MCDHF/RCI}}$	$gf_{\text{MCDHF/RCI}}$	$A_{\text{MCDHF/RCI}}$	BR
10	3	1	8.95657E+02	E1	2.016E-05	6.837E-06	1.895E+04	1.000E+00
10	4	1	8.87759E+02	M2	1.059E+01	3.384E-11	5.728E-02	8.126E-01
10	4	3	1.00669E+05	M1	2.499E+00	1.004E-07	1.321E-02	1.874E-01
10	5	1	4.64974E+02	E1	5.935E-01	3.877E-01	3.988E+09	1.000E+00
10	6	3	5.63031E+02	E1	2.711E-01	1.463E-01	3.078E+09	1.000E+00
10	6	5	1.34781E+03	E1	3.803E-05	8.572E-06	3.147E+04	1.023E-05
10	7	2	5.59992E+02	E1	2.714E-01	1.472E-01	1.044E+09	3.377E-01
10	7	3	5.61414E+02	E1	2.035E-01	1.101E-01	7.766E+08	2.512E-01
10	7	4	5.64563E+02	E1	3.386E-01	1.822E-01	1.271E+09	4.111E-01
10	8	3	5.58649E+02	E1	3.394E-01	1.846E-01	7.889E+08	2.535E-01
10	8	4	5.61766E+02	E1	1.016E+00	5.496E-01	2.323E+09	7.465E-01
10	8	5	1.32297E+03	E1	6.271E-04	1.440E-04	1.097E+05	3.526E-05
10	9	3	4.85279E+02	E1	5.070E-05	3.173E-05	1.798E+05	3.256E-04
10	9	4	4.87630E+02	E1	7.130E-04	4.441E-04	2.492E+06	4.513E-03
10	9	5	9.74172E+02	E1	1.253E+00	3.908E-01	5.494E+08	9.952E-01
10	10	3	3.55024E+02	E1	4.570E-06	3.910E-06	2.069E+05	3.661E-05
10	10	5	5.60992E+02	E1	4.925E-01	2.667E-01	5.652E+09	1.000E+00
10	11	2	1.15340E+02	E1	1.409E-02	3.710E-02	6.201E+09	1.109E-01

*Table 5 continued*

**Table 5** (*continued*)

$Z$	$j$	$i$	$\lambda_{\text{MCDHF/RCI}}$	Type	$S_{\text{MCDHF/RCI}}$	$gf_{\text{MCDHF/RCI}}$	$A_{\text{MCDHF/RCI}}$	BR
10	11	3	1.15400E+02	E1	4.238E-02	1.116E-01	1.863E+10	3.331E-01
10	11	4	1.15533E+02	E1	7.100E-02	1.867E-01	3.110E+10	5.560E-01
10	11	5	1.31039E+02	E1	2.828E-06	6.555E-06	8.488E+05	1.518E-05
10	12	3	1.12807E+02	E1	1.756E-07	4.728E-07	2.478E+05	1.378E-05
10	12	5	1.27705E+02	E1	1.849E-02	4.398E-02	1.799E+10	1.000E+00
10	12	9	1.46972E+02	E2	2.230E-02	1.180E-06	3.642E+05	2.025E-05
10	13	1	9.75090E+01	E1	1.558E-01	4.855E-01	1.135E+11	9.425E-01
10	13	5	1.23384E+02	E2	1.721E-01	1.538E-05	2.246E+06	1.865E-05
10	13	8	1.36074E+02	E1	3.692E-05	8.242E-05	9.897E+06	8.216E-05
10	13	9	1.41277E+02	E1	2.761E-02	5.937E-02	6.614E+09	5.490E-02
10	13	10	1.58172E+02	E1	1.616E-03	3.104E-03	2.758E+08	2.290E-03
10	13	12	3.64580E+03	E1	1.910E+00	1.592E-01	2.662E+07	2.210E-04
10	14	4	1.09215E+02	E2	8.565E-02	1.104E-05	6.174E+06	1.085E-02
10	14	7	1.35411E+02	E1	4.387E-04	9.840E-04	3.580E+08	6.292E-01
10	14	11	1.99729E+03	E1	8.051E-01	1.224E-01	2.047E+08	3.599E-01
10	15	1	9.72386E+01	E1	5.497E-04	1.717E-03	4.038E+08	4.031E-01
10	15	3	1.09081E+02	E2	6.383E-02	8.257E-06	1.543E+06	1.540E-03
10	15	4	1.09200E+02	E2	1.918E-01	2.473E-05	4.611E+06	4.604E-03
10	15	6	1.35293E+02	E1	4.478E-04	1.005E-03	1.221E+08	1.219E-01
10	15	7	1.35386E+02	E1	3.234E-04	7.255E-04	8.801E+07	8.786E-02
10	15	8	1.35548E+02	E1	5.366E-04	1.203E-03	1.455E+08	1.453E-01
10	15	9	1.40710E+02	E1	1.219E-04	2.631E-04	2.954E+07	2.950E-02
10	15	10	1.57461E+02	E1	4.182E-06	8.068E-06	7.235E+05	7.223E-04
10	15	11	1.99202E+03	E1	2.407E+00	3.671E-01	2.057E+08	2.053E-01
10	15	12	3.30247E+03	E1	7.105E-03	6.535E-04	1.332E+05	1.330E-04
10	16	2	1.08997E+02	E2	8.510E-02	1.103E-05	1.239E+06	2.119E-03
10	16	3	1.09051E+02	E2	1.917E-01	2.482E-05	2.784E+06	4.761E-03
10	16	4	1.09169E+02	E2	1.495E-01	1.929E-05	2.160E+06	3.693E-03
10	16	7	1.35340E+02	E1	5.798E-04	1.301E-03	9.478E+07	1.621E-01
10	16	8	1.35502E+02	E1	1.682E-03	3.771E-03	2.740E+08	4.685E-01
10	16	9	1.40660E+02	E1	7.032E-07	1.518E-06	1.024E+05	1.751E-04
10	16	11	1.98202E+03	E1	4.030E+00	6.176E-01	2.097E+08	3.587E-01
10	17	2	1.06042E+02	E1	2.368E-01	6.782E-01	1.341E+11	5.557E-01
10	17	3	1.06093E+02	E1	1.777E-01	5.087E-01	1.005E+11	4.164E-01
10	17	4	1.06204E+02	E1	1.187E-02	3.394E-02	6.691E+09	2.773E-02
10	17	5	1.19167E+02	E1	8.574E-06	2.186E-05	3.422E+06	1.418E-05
10	17	14	3.85233E+03	E1	1.084E+00	8.545E-02	1.280E+07	5.306E-05
10	17	15	3.87212E+03	E1	8.095E-01	6.351E-02	9.418E+06	3.903E-05
10	18	3	1.06088E+02	E1	5.327E-01	1.525E+00	1.808E+11	7.502E-01
10	18	4	1.06200E+02	E1	1.779E-01	5.088E-01	6.018E+10	2.497E-01
10	18	15	3.86602E+03	E1	2.430E+00	1.909E-01	1.704E+07	7.071E-05
10	18	16	3.90422E+03	E1	8.128E-01	6.324E-02	5.535E+06	2.296E-05
10	19	4	1.06192E+02	E1	9.952E-01	2.847E+00	2.406E+11	9.999E-01
10	19	16	3.89309E+03	E1	4.559E+00	3.557E-01	2.236E+07	9.296E-05
10	20	1	9.32952E+01	E2	9.371E-01	1.938E-04	2.970E+07	1.921E-04
10	20	3	1.04143E+02	E1	6.061E-06	1.768E-05	2.175E+06	1.406E-05
10	20	5	1.16713E+02	E1	6.059E-01	1.577E+00	1.544E+11	9.989E-01
10	20	13	2.15887E+03	E1	3.456E+00	4.863E-01	1.392E+08	9.003E-04

Table 5 is published in its entirety in the machine-readable format. A portion is shown here for guidance regarding its form and content.

**Table 6.** The differences in % of line strengths  $S$  (in length form) for the transitions among the lowest 20 levels up to the  $2s3d$  configuration of Ne VII from different resources, MCDHF/RCI (AS<sub>4</sub>), MCHF/BP, and NIST, relative to the values of the present MCDHF/RCI (AS<sub>5</sub>) calculations. Radiative branching ratios (BR) for each transition from the present MCDHF/RCI (AS<sub>5</sub>) calculations are listed in the last column. MCDHF/RCI (AS<sub>4</sub>) - the present MCDHF/RCI values of the AS<sub>4</sub> active set; MCDHF/RCI (AS<sub>5</sub>) - the present MCDHF/RCI values of the AS<sub>5</sub> active set; MCHF/BP - the values provided by Tachiev & Froese Fischer (1999); Froese Fischer & Tachiev (2004); NIST -the values included in the NIST ASD, as well as the estimated accuracies of transition data using the terminology of the NIST ASD (Kramida et al. 2016).

Upper level	Lower level	Type	MCDHF/RCI		NIST	Differences (%)			BR	
			AS <sub>4</sub>	AS <sub>5</sub>		AS <sub>4</sub>	MCHF/BP	NIST		
$2s2p\ ^3P_1^o$	$2s^2\ ^1S_0$	E1	2.01E-05	2.02E-05	2.04E-05	1.90E-05 <sup>C</sup>	-0.3	1.0	-5.8	1.00E+00
$2s2p\ ^3P_2^o$	$2s^2\ ^1S_0$	M2	1.06E+01	1.06E+01	1.06E+01	1.06E+01 <sup>A</sup>	0.0	-0.2	0.1	8.13E-01
$2s2p\ ^3P_2^o$	$2s2p\ ^3P_1^o$	M1	2.50E+00	2.50E+00	2.50E+00	2.50E+00 <sup>B</sup>	0.0	0.0	0.0	1.87E-01
$2s2p\ ^1P_1^o$	$2s^2\ ^1S_0$	E1	5.93E-01	5.94E-01	5.94E-01	5.86E-01 <sup>A</sup>	-0.1	0.0	-1.3	1.00E+00
$2p^2\ ^3P_0$	$2s2p\ ^3P_1^o$	E1	2.71E-01	2.71E-01	2.71E-01	2.72E-01 <sup>A</sup>	0.0	0.0	0.3	1.00E+00
$2p^2\ ^3P_0$	$2s2p\ ^1P_1^o$	E1	3.78E-05	3.80E-05	3.87E-05	3.80E-05 <sup>D</sup>	-0.5	1.7	-0.1	1.02E-05
$2p^2\ ^3P_1$	$2s2p\ ^3P_0^o$	E1	2.71E-01	2.71E-01	2.71E-01	2.73E-01 <sup>A</sup>	0.0	-0.1	0.6	3.38E-01
$2p^2\ ^3P_1$	$2s2p\ ^3P_1^o$	E1	2.04E-01	2.04E-01	2.03E-01	2.04E-01 <sup>A</sup>	0.0	-0.1	0.2	2.51E-01
$2p^2\ ^3P_1$	$2s2p\ ^3P_2^o$	E1	3.39E-01	3.39E-01	3.39E-01	3.40E-01 <sup>A</sup>	0.0	0.1	0.4	4.11E-01
$2p^2\ ^3P_2$	$2s2p\ ^3P_1^o$	E1	3.39E-01	3.39E-01	3.39E-01	3.41E-01 <sup>A</sup>	0.0	-0.1	0.5	2.54E-01
$2p^2\ ^3P_2$	$2s2p\ ^3P_2^o$	E1	1.02E+00	1.02E+00	1.02E+00	1.02E+00 <sup>A</sup>	0.0	0.0	0.4	7.47E-01
$2p^2\ ^3P_2$	$2s2p\ ^1P_1^o$	E1	6.22E-04	6.27E-04	6.28E-04	6.00E-04 <sup>C</sup>	-0.7	0.1	-4.3	3.53E-05
$2p^2\ ^1D_2$	$2s2p\ ^3P_1^o$	E1	5.01E-05	5.07E-05	5.53E-05	4.49E-05 <sup>A</sup>	-1.2	9.2	-11.4	3.26E-04
$2p^2\ ^1D_2$	$2s2p\ ^3P_2^o$	E1	7.08E-04	7.13E-04	7.04E-04	6.80E-04 <sup>A</sup>	-0.7	-1.3	-4.6	4.51E-03
$2p^2\ ^1D_2$	$2s2p\ ^1P_1^o$	E1	1.25E+00	1.25E+00	1.25E+00	1.27E+00 <sup>B</sup>	0.1	0.0	1.4	9.95E-01
$2p^2\ ^1S_0$	$2s2p\ ^3P_1^o$	E1	4.52E-06	4.57E-06	4.58E-06	3.92E-06 <sup>A</sup>	-1.0	0.3	-14.2	3.66E-05
$2p^2\ ^1S_0$	$2s2p\ ^1P_1^o$	E1	4.93E-01	4.93E-01	4.92E-01	4.87E-01 <sup>A</sup>	0.0	-0.1	-1.1	1.00E+00
$2s3s\ ^3S_1$	$2s2p\ ^3P_0^o$	E1	1.41E-02	1.41E-02	1.41E-02	1.44E-02 <sup>A</sup>	0.0	0.1	2.2	1.11E-01
$2s3s\ ^3S_1$	$2s2p\ ^3P_1^o$	E1	4.24E-02	4.24E-02	4.24E-02	4.33E-02 <sup>A</sup>	0.0	0.0	2.2	3.33E-01
$2s3s\ ^3S_1$	$2s2p\ ^3P_2^o$	E1	7.10E-02	7.10E-02	7.10E-02	7.26E-02 <sup>A</sup>	0.0	0.0	2.3	5.56E-01
$2s3s\ ^3S_1$	$2s2p\ ^1P_1^o$	E1	2.83E-06	2.83E-06	3.47E-06	2.80E-06 <sup>B</sup>	0.2	22.7	-1.0	1.52E-05
$2s3s\ ^1S_0$	$2s2p\ ^3P_1^o$	E1	1.75E-07	1.76E-07	...	1.85E-07 <sup>E</sup>	-0.3	...	5.4	1.38E-05
$2s3s\ ^1S_0$	$2s2p\ ^1P_1^o$	E1	1.86E-02	1.85E-02	...	1.50E-02 <sup>C</sup>	0.5	...	-18.9	1.00E+00
$2s3s\ ^1S_0$	$2p^2\ ^1D_2$	E2	2.26E-02	2.23E-02	...	...	1.4	...	...	2.03E-05
$2s3p\ ^1P_1^o$	$2s^2\ ^1S_0$	E1	1.56E-01	1.56E-01	1.56E-01	1.56E-01 <sup>A</sup>	-0.1	0.2	0.1	9.43E-01
$2s3p\ ^1P_1^o$	$2s2p\ ^1P_1^o$	E2	1.73E-01	1.72E-01	...	...	0.4	...	...	1.87E-05
$2s3p\ ^1P_1^o$	$2p^2\ ^3P_2$	E1	3.71E-05	3.69E-05	3.71E-05	3.50E-05 <sup>D</sup>	0.5	0.4	-5.2	8.22E-05
$2s3p\ ^1P_1^o$	$2p^2\ ^1D_2$	E1	2.79E-02	2.76E-02	2.71E-02	2.00E-02 <sup>D</sup>	0.9	-1.8	-27.6	5.49E-02
$2s3p\ ^1P_1^o$	$2p^2\ ^1S_0$	E1	1.63E-03	1.62E-03	1.63E-03	1.63E-03 <sup>B</sup>	0.6	1.0	0.9	2.29E-03
$2s3p\ ^1P_1^o$	$2s3s\ ^1S_0$	E1	1.91E+00	1.91E+00	...	1.88E+00 <sup>B</sup>	0.1	...	-1.6	2.21E-04
$2s3p\ ^3P_0^o$	$2s2p\ ^3P_2^o$	E2	8.57E-02	8.57E-02	...	...	0.1	...	...	1.09E-02
$2s3p\ ^3P_0^o$	$2p^2\ ^3P_1$	E1	4.39E-04	4.39E-04	4.29E-04	4.50E-04 <sup>C</sup>	0.0	-2.3	2.6	6.29E-01
$2s3p\ ^3P_0^o$	$2s3s\ ^3S_1$	E1	8.06E-01	8.05E-01	8.05E-01	8.07E-01 <sup>A</sup>	0.0	0.0	0.2	3.60E-01
$2s3p\ ^3P_1^o$	$2s^2\ ^1S_0$	E1	5.59E-04	5.50E-04	5.66E-04	8.40E-04 <sup>A</sup>	1.7	3.0	52.8	4.03E-01
$2s3p\ ^3P_1^o$	$2s2p\ ^3P_1^o$	E2	6.39E-02	6.38E-02	...	...	0.1	...	...	1.54E-03
$2s3p\ ^3P_1^o$	$2s2p\ ^3P_2^o$	E2	1.92E-01	1.92E-01	...	...	0.1	...	...	4.60E-03
$2s3p\ ^3P_1^o$	$2p^2\ ^3P_0$	E1	4.48E-04	4.48E-04	4.40E-04	4.40E-04 <sup>C</sup>	0.0	-1.9	-1.7	1.22E-01
$2s3p\ ^3P_1^o$	$2p^2\ ^3P_1$	E1	3.23E-04	3.23E-04	3.26E-04	3.30E-04 <sup>C</sup>	-0.1	0.8	2.0	8.79E-02

Table 6 continued

**Table 6** (*continued*)

Upper level	Lower level	Type	MCDHF/RCI		MCHF/BP	NIST	Differences (%)			BR
			AS <sub>4</sub>	AS <sub>5</sub>			AS <sub>4</sub>	MCHF/BP	NIST	
2s3p <sup>3</sup> P <sub>1</sub> <sup>o</sup>	2p <sup>2</sup> <sup>3</sup> P <sub>2</sub>	E1	5.36E-04	5.37E-04	5.24E-04	5.30E-04 <sup>C</sup>	-0.1	-2.4	-1.2	1.45E-01
2s3p <sup>3</sup> P <sub>1</sub> <sup>o</sup>	2p <sup>2</sup> <sup>1</sup> D <sub>2</sub>	E1	1.25E-04	1.22E-04	1.30E-04	1.20E-04 <sup>D</sup>	2.5	6.6	-1.6	2.95E-02
2s3p <sup>3</sup> P <sub>1</sub> <sup>o</sup>	2p <sup>2</sup> <sup>1</sup> S <sub>0</sub>	E1	4.30E-06	4.18E-06	4.36E-06	4.36E-06 <sup>D</sup>	2.9	4.2	4.3	7.22E-04
2s3p <sup>3</sup> P <sub>1</sub> <sup>o</sup>	2s3s <sup>3</sup> S <sub>1</sub>	E1	2.41E+00	2.41E+00	2.41E+00	2.41E+00 <sup>A</sup>	0.0	0.0	0.1	2.05E-01
2s3p <sup>3</sup> P <sub>1</sub> <sup>o</sup>	2s3s <sup>1</sup> S <sub>0</sub>	E1	7.24E-03	7.11E-03	...	1.07E-02 <sup>A</sup>	1.9	...	50.6	1.33E-04
2s3p <sup>3</sup> P <sub>2</sub> <sup>o</sup>	2s2p <sup>3</sup> P <sub>0</sub> <sup>o</sup>	E2	8.52E-02	8.51E-02	...	...	0.1	...	...	2.12E-03
2s3p <sup>3</sup> P <sub>2</sub> <sup>o</sup>	2s2p <sup>3</sup> P <sub>1</sub> <sup>o</sup>	E2	1.92E-01	1.92E-01	...	...	0.1	...	...	4.76E-03
2s3p <sup>3</sup> P <sub>2</sub> <sup>o</sup>	2s2p <sup>3</sup> P <sub>2</sub> <sup>o</sup>	E2	1.50E-01	1.50E-01	...	...	0.1	...	...	3.69E-03
2s3p <sup>3</sup> P <sub>2</sub> <sup>o</sup>	2p <sup>2</sup> <sup>3</sup> P <sub>1</sub>	E1	5.80E-04	5.80E-04	5.71E-04	5.40E-04 <sup>C</sup>	0.0	-1.5	-6.9	1.62E-01
2s3p <sup>3</sup> P <sub>2</sub> <sup>o</sup>	2p <sup>2</sup> <sup>3</sup> P <sub>2</sub>	E1	1.68E-03	1.68E-03	1.69E-03	1.60E-03 <sup>C</sup>	-0.1	0.7	-4.9	4.69E-01
2s3p <sup>3</sup> P <sub>2</sub> <sup>o</sup>	2p <sup>2</sup> <sup>1</sup> D <sub>2</sub>	E1	6.97E-07	7.03E-07	7.88E-07	3.40E-07 <sup>C</sup>	-1.0	12.0	-51.6	1.75E-04
2s3p <sup>3</sup> P <sub>2</sub> <sup>o</sup>	2s3s <sup>3</sup> S <sub>1</sub>	E1	4.03E+00	4.03E+00	4.03E+00	4.00E+00 <sup>B</sup>	0.0	0.0	-0.7	3.59E-01
2s3d <sup>3</sup> D <sub>1</sub>	2s2p <sup>3</sup> P <sub>0</sub> <sup>o</sup>	E1	2.37E-01	2.37E-01	2.37E-01	2.40E-01 <sup>A</sup>	-0.1	0.0	1.4	5.56E-01
2s3d <sup>3</sup> D <sub>1</sub>	2s2p <sup>3</sup> P <sub>1</sub> <sup>o</sup>	E1	1.78E-01	1.78E-01	1.78E-01	1.80E-01 <sup>A</sup>	-0.1	0.0	1.3	4.16E-01
2s3d <sup>3</sup> D <sub>1</sub>	2s2p <sup>3</sup> P <sub>2</sub> <sup>o</sup>	E1	1.19E-02	1.19E-02	1.19E-02	1.20E-02 <sup>A</sup>	-0.1	-0.1	1.1	2.77E-02
2s3d <sup>3</sup> D <sub>1</sub>	2s2p <sup>1</sup> P <sub>1</sub> <sup>o</sup>	E1	8.55E-06	8.57E-06	1.07E-05	9.20E-06 <sup>A</sup>	-0.3	24.9	7.3	1.42E-05
2s3d <sup>3</sup> D <sub>1</sub>	2s3p <sup>3</sup> P <sub>0</sub> <sup>o</sup>	E1	1.09E+00	1.08E+00	1.08E+00	1.09E+00 <sup>A</sup>	0.1	0.0	0.6	5.31E-05
2s3d <sup>3</sup> D <sub>1</sub>	2s3p <sup>3</sup> P <sub>1</sub> <sup>o</sup>	E1	8.10E-01	8.10E-01	8.10E-01	8.13E-01 <sup>A</sup>	0.1	0.0	0.4	3.90E-05
2s3d <sup>3</sup> D <sub>2</sub>	2s2p <sup>3</sup> P <sub>1</sub> <sup>o</sup>	E1	5.32E-01	5.33E-01	5.33E-01	5.40E-01 <sup>A</sup>	-0.1	0.0	1.4	7.50E-01
2s3d <sup>3</sup> D <sub>2</sub>	2s2p <sup>3</sup> P <sub>2</sub> <sup>o</sup>	E1	1.78E-01	1.78E-01	1.78E-01	1.80E-01 <sup>A</sup>	-0.1	-0.1	1.2	2.50E-01
2s3d <sup>3</sup> D <sub>2</sub>	2s3p <sup>3</sup> P <sub>1</sub> <sup>o</sup>	E1	2.43E+00	2.43E+00	2.43E+00	2.44E+00 <sup>A</sup>	0.1	0.0	0.4	7.07E-05
2s3d <sup>3</sup> D <sub>2</sub>	2s3p <sup>3</sup> P <sub>2</sub> <sup>o</sup>	E1	8.14E-01	8.13E-01	8.13E-01	8.19E-01 <sup>A</sup>	0.1	0.0	0.8	2.30E-05
2s3d <sup>3</sup> D <sub>3</sub>	2s2p <sup>3</sup> P <sub>2</sub> <sup>o</sup>	E1	9.94E-01	9.95E-01	9.95E-01	1.01E+00 <sup>A</sup>	-0.1	0.0	1.5	1.00E+00
2s3d <sup>3</sup> D <sub>3</sub>	2s3p <sup>3</sup> P <sub>2</sub> <sup>o</sup>	E1	4.56E+00	4.56E+00	4.56E+00	4.59E+00 <sup>A</sup>	0.1	0.1	0.7	9.30E-05
2s3d <sup>1</sup> D <sub>2</sub>	2s <sup>2</sup> <sup>1</sup> S <sub>0</sub>	E2	9.38E-01	9.37E-01	...	...	0.1	...	...	1.92E-04
2s3d <sup>1</sup> D <sub>2</sub>	2s2p <sup>3</sup> P <sub>1</sub> <sup>o</sup>	E1	6.09E-06	6.06E-06	6.25E-06	5.50E-06 <sup>B</sup>	0.4	3.1	-9.3	1.41E-05
2s3d <sup>1</sup> D <sub>2</sub>	2s2p <sup>1</sup> P <sub>1</sub> <sup>o</sup>	E1	6.07E-01	6.06E-01	6.05E-01	5.88E-01 <sup>A</sup>	0.2	-0.1	-3.0	9.99E-01
2s3d <sup>1</sup> D <sub>2</sub>	2s3p <sup>1</sup> P <sub>1</sub> <sup>o</sup>	E1	3.45E+00	3.46E+00	3.46E+00	3.45E+00 <sup>A</sup>	-0.1	0.1	-0.2	9.00E-04

**Table 7.** Comparisons between the experimental and theoretical lifetimes (in s) for the  $2s2p\ ^{1,3}P_1^{\circ}$  levels of the ions from B II to Ne VII.

Z	Key	State	Exp. <sup>a</sup>	Uncertainty <sup>a</sup>	MCDHF/RCI <sup>b</sup>	MCDHF/RCI <sup>c</sup>	RCI <sup>d</sup>
5	3	$2s2p\ ^3P_1^{\circ}$	9.765E-02 <sup>[e]</sup>	0.05E-02	9.513E-02	...	...
6	3	$2s2p\ ^3P_1^{\circ}$	9.714E-03 <sup>[f]</sup>	0.013E-03	9.795E-03	...	9.970E-03
7	3	$2s2p\ ^3P_1^{\circ}$	1.73E-03 <sup>[g]</sup>	0.01E-03	1.751E-03	1.790E-03	1.766E-03
8	3	$2s2p\ ^3P_1^{\circ}$	4.32E-04 <sup>[g]</sup>	0.09E-04	4.440E-04	4.521E-04	4.462E-04
9	3	$2s2p\ ^3P_1^{\circ}$	...	...	1.437E-04	1.418E-04	
10	3	$2s2p\ ^3P_1^{\circ}$	4.5E-05 <sup>[h]</sup>	2.3E-05	5.277E-05	5.371E-05	5.299E-05
5	5	$2s2p\ ^1P_1^{\circ}$	8.6E-10 <sup>[i]</sup>	0.7E-10	8.285E-10	...	...
6	5	$2s2p\ ^1P_1^{\circ}$	5.7E-10 <sup>[j]</sup>	0.2E-10	5.634E-10	...	5.672E-10
7	5	$2s2p\ ^1P_1^{\circ}$	4.25E-10 <sup>[k]</sup>	0.15E-10	4.299E-10	4.285E-10	4.316E-10
8	5	$2s2p\ ^1P_1^{\circ}$	3.38E-10 <sup>[k]</sup>	0.15E-10	3.480E-10	3.466E-10	3.490E-10
9	5	$2s2p\ ^1P_1^{\circ}$	3.1E-10 <sup>[l]</sup>	0.4E-10	2.919E-10	2.907E-10	2.925E-10
10	5	$2s2p\ ^1P_1^{\circ}$	2.32E-10 <sup>[m]</sup>	0.37E-10	2.508E-10	2.498E-10	2.511E-10

<sup>a</sup> Experimental lifetimes and experimental uncertainties.

<sup>b</sup> The present MCDHF/RCI lifetimes.

<sup>c</sup> The MCDHF/RCI lifetimes calculated by Jönsson et al. (1998).

<sup>d</sup> The RCI lifetimes calculated by Cheng et al. (2008).

The experimental lifetimes from Träbert et al. (1999)<sup>[e]</sup>, Doerfert et al. (1997)<sup>[f]</sup>, Träbert et al. (2005)<sup>[g]</sup>, Kunze (1972)<sup>[h]</sup>, Bashkin et al. (1985)<sup>[i]</sup>, Reistad et al. (1986)<sup>[j]</sup>, Engström et al. (1981)<sup>[k]</sup>, Knystautas et al. (1979)<sup>[l]</sup>, and Irwin et al. (1973)<sup>[m]</sup>.